NASA Contractor Report 179609
FCR-8347

# Regenerative Fuel Cell Study for Satellites in GEO Orbit

Alexander Levy, Leslie L. Van Dine,
and James K. Stedman
*International Fuel Cells Corporation*
*South Windsor, Connecticut*

July 1987

Prepared for
Lewis Research Center
Under Contract NAS3-22234

(NASA-CR-179609) REGENERATIVE FUEL CELL STUDY FOR SATELLITES IN GEO ORBIT Final Contractor Report (International Fuel Cells Corp.) 82 p Avail: NTIS HC A05/MF A01
CSCL 10B G3/44
N87-27324
Unclas
0087885

National Aeronautics and
Space Administration

# FOREWORD

The final report describes the work completed under Task XIV of the Long-Life, High Performance Fuel Cell Program, NASA Contract No. NAS3-22234 from 1 November 1984 through October 1986 by International Fuel Cells Corporation.

The NASA Task Manager for this contract was Ms. Olga Gonzalez-Sanabria. The contributions of Ms. Gozalez-Sanabria and Dr. Lawrence H. Thaller of the NASA Research Center are gratefully acknowledged.

The Task Manager for International Fuel Cells was Mr. Alex Levy. Other International Fuel Cell personnel who were involved in this study were James K. Stedman, Leslie L. Van Dine and John Trocciola.

# TABLE OF CONTENTS

Page

TABLE OF CONTENTS (Cont'd)

# I. SUMMARY

## A. Objectives and Scope of Study

This final report summarizes the results of a 12 month study performed by International Fuel Cells (IFC) for the NASA Lewis Research Center under Contract NAS3-22234 - Task XIV. The study objective was to identify high performance regenerative $H_2$-$O_2$ fuel cell systems which could be competitive with advanced high energy rechargeable batteries such as Ni-$H_2$ and NA-S for geosynchronous (GEO) satellite missions. Extrapolation of this technology to be suitable for middle earth orbit (MEO) application was also conducted. A requirement for a technology readiness date of 1988 to 1992 was assumed in formulating system concepts.

The mission requirements and performance goals were specified by NASA for both GEO and MEO applications and are described in the table below:

| | MEO | GEO |
|---|---|---|
| • MAX. REQ'D POWER, kW | 50 | 25 |
| • AVG. POWER, kW | 18.4 | 25 |
| • NOMINAL VOLTAGE AT DISCHARGE, VOLTS | 180 | 120 |
| • CHARGE/DISCHARGE TIME RATIO, HRS/HRS | 3/3 | 22.8/1.2 |
| • DESIGN CYCLE LIFE | 7500 | 1000 |
| • DESIGN LIFE, YRS. | 5 | 10 |
| • DESIGN ENERGY STORAGE, W-HRS | 55,000 | 30,000 |
| • MODULE ENERGY DENSITY GOAL, W-HRS/LB. | 30 | 50 |
| • EFFICIENCY GOAL | 55 | 55 |
| • RELIABILITY | UNMANNED<br>(.995) | |

Previous studies of regenerative fuel cell systems have indicated that due to the need for dynamic components for thermal, reactant, and product control, the achievement of the reliability levels required for unmanned missions of up to ten years requires a high degree of redundancy resulting in reduced energy density. Based on the need for high reliability and high specific energy density, a number of system concepts were studied which minimized the dynamic components, and emphasized passive means for water transfer, heat management and system control.

Two fuel cell types were studied. Primary emphasis was placed on the alkaline electrolyte fuel cell because of its high performance, advanced state of development, and proven ability to operate in a launch and space environment. The second fuel cell type which was studied utilized a polymer electrolyte membrane (PEM). This cell has been used previously on the Gemini and other space programs. The PEM cell generally has lower performance than that of the alkaline and suffers from a coulombic loss caused by reactant gas diffusion through the membranes. On the positive side, the PEM cell specific weight (lbs./ft$^2$) is lower than that for an alkaline cell.

Three alkaline system configurations were studied. The first, termed the "integrated" design, utilized a configuration in which the fuel cells and electrolysis cells are annular in shape and are alternately stacked inside a pressure vessel. Product water is stored in porous plates and transferred by diffusion during electrolysis operation. Waste heat is conducted to a graphite plate located between cell pairs and then conducted through the radial plane of the plate to the pressure vessel wall.

One advantage of this design lies in the relative ease of heat and water management due to the intimate arrangement of both fuel cell and electrolysis cells. In addition, when the system is operated at elevated pressure, it is possible to store both hydrogen and oxygen reactant gases in the same pressure vessel as the cell stack, thus eliminating the need for providing gas penetrations into the vessel, resulting in improved reliability.

The second alkaline system studied, which is referred to as the "dedicated" design uses a separate fuel cell and electrolysis stack. In this approach each stack can be more optimally designed in terms of individual cell area and number of cells required. Also, each stack may be operated at a fixed pressure, so that performance during the charge or discharge cycle is a constant value. The electrolysis cell was assumed to be encapsulated in a containment vessel because of its elevated operating pressure.

The final alkaline system assumed a "dual function" configuration. That is a stack consisting of single cells which can operate in both the fuel cell and electrolysis mode. To date it has not been possible to find high performance oxygen electrodes that can operate stably over the range for voltage levels required. For this study a parametric approach both to fuel cell performance and cell and cooler specific weight (lbs./ft$^2$) was taken to establish the impact of these parameters on specific energy density. This configuration offers a number of advantages, such as minimizing the number of cells required which results in added reliability; ease of heat and water management; bipolar current collection and the potential, if operated at high pressure, to contain the cell stack and reactant gases in a single pressure vessel. The major disadvantage of course, is the need to find a stable oxygen catalyst, for which the fuel cell performance is not sufficiently depressed, to cause this system to be unattractive from a specific energy viewpoint.

The PEM system studied was of a dedicated design, using separate PEM cells for the fuel cell and electrolysis stack. The incentive for studying this system lies in the low specific weight for each cell (lbs/ft$^2$). The performance, however, is somewhat lower than that of an alkaline system. In addition, the PEM membrane tends to permit diffusion of the reactant gases, resulting in a non-productive reaction of the hydrogen and oxygen. This parasitic reaction occurs to some extent at all times, but losses become substantial when the pressure is high and the operating current is low. In the PEM design, it was assumed that liquid water produced at the fuel cell cathode would be transferred through a membrane between cells and vaporized by the cell waste heat (similar to the dedicated alkaline system.) The water vapor leaving the fuel cell is fed directly to the electrolysis cell by a pressure differential, where the vapor is condensed and stored in a porous plate at the cathode ($H_2$ electrode).

## B. Results

The major results of this study are shown in Figure S-1 which depicts the energy density for each option described above. The analysis was done for an overall system efficiency of 55% with the satellite in a geosynchronous orbit. The specific energy densities shown in Figure S-1 are at a single power plant module level and do not include redundant modules required to achieve a desired level of reliability. The major conclusions that can be drawn from this study are as follows:

- The regenerable systems studied indicate that energy densities competitive with advanced batteries are possible, with the use of relatively near term technology. Extrapolation of advanced alkaline regenerable systems show a potential improvement in energy density by approximately a factor of two over Na-S batteries.

- For the first three options shown in Figure S-1 where low reactant storage pressure (i.e. 300 psia) is assumed, the energy density variation was between 36.9 and 41.3 whrs/lb. This includes reactants, tankage, electrolysis and fuel cell stacks containment vessels, controls, heat exchangers and support structure. The twelve percent variation in specific energy is not considered significant to the level of detail used in the study.

- At low electrolysis pressure (300 psia) all the containment tanks were assumed to be metal (Inconel 718), since consultation with SCI, Inc., a tank manufacturer, indicated that at low pressure levels, composite tankage would not affect a weight savings.

- Raising the storage pressure of the first three options to 1800 psia and using 6061-T6 aluminum liner overwrapped with carbon epoxy composite material for all tankage, results in energy densities between 46.0 and 50.0 Whrs/lb or a gain over low pressure storage of 23 percent.

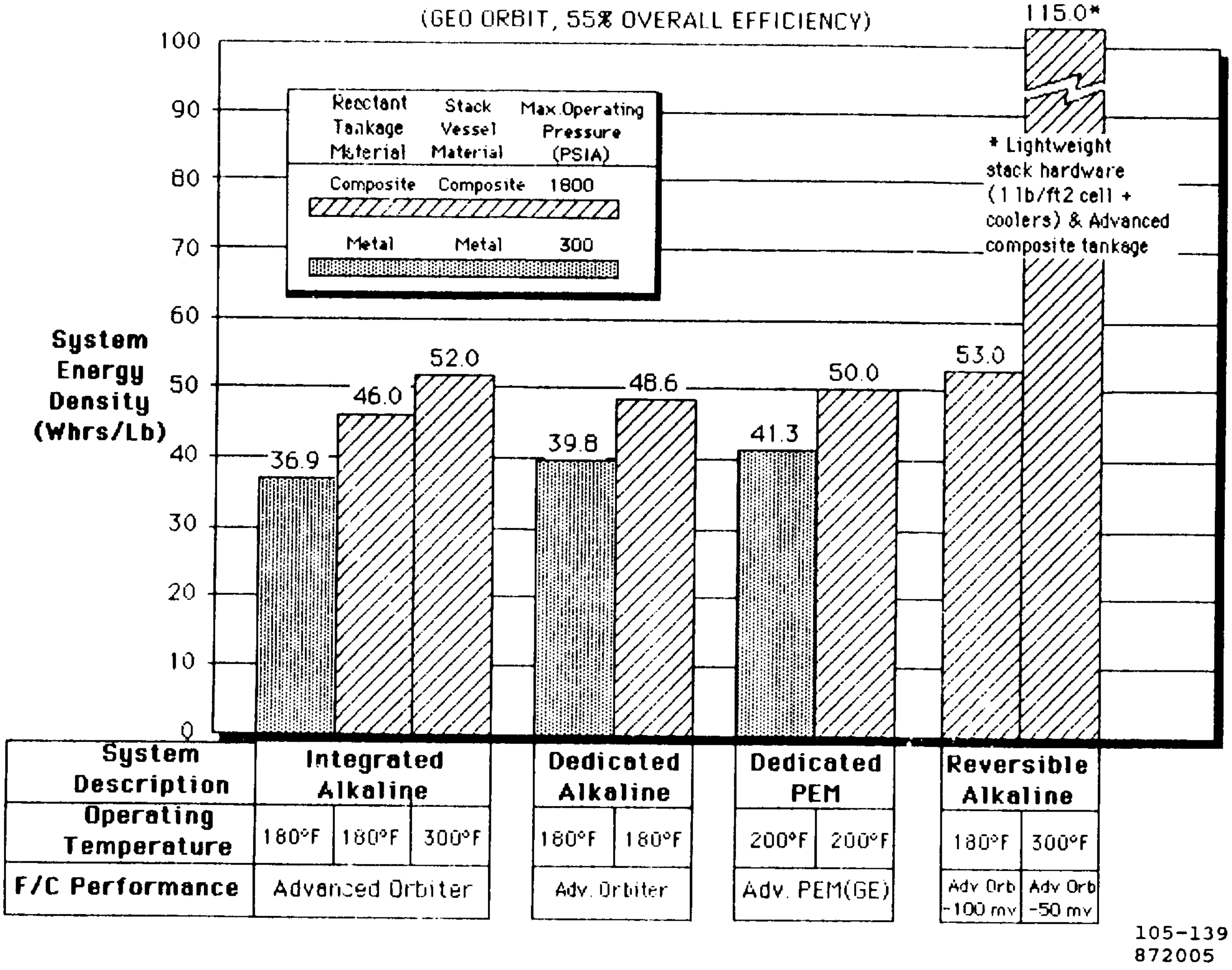

Figure S-1. Energy Density Results for Systems Studied

- High pressure storage of reactants has a dramatic effect on system specific volume. Increasing pressure from 300 to 1800 psia reduces module specific volume from 2.75 ft$^3$/kW to .51 ft$^3$/kW for the integrated alkaline system.

- For the same system, if both pressure and temperature are increased (from 300 to 1800 psia and from 180°F to 300°F) the specific energy density increases to 52 W-hrs/lb., or an increase of 41 percent over the baseline design (36.9 W-hrs/lb).

- Another interesting conclusion is that for the equipment listed above, the maximum energy density does not occur at the goal 55% efficiency, but reaches a maximum at about 50% (see Figure 22). This optimization point may vary depending on the weight of the external cooling system, radiator and solar cells. It is probable that when this equipment is added into the total, the optimization will occur at a higher efficiency, since each of these elements would tend to get lower in weight as efficiency increases.

- Results of a study of the integrated alkaline system for MEO application indicates energy densities very comparable to the GEO values, 35.7 vs. 36.9 W-hrs/lb. Trade studies showing the influence of tankage material, pressure and temperature for the MEO application were not conducted, but it is reasonable to assume similar benefits can be made.

- The most attractive option utilizes reversible cells. As shown in Figure S-1, even if the fuel cell performance is reduced by 100 mV from present levels, the system specific energy would be 53.0 W-hrs/lb. At the present time programs are under way to reduce the specific weight of alkaline cells. Designs as low as .34 lbs/ft$^2$ have been conceived. A reasonable assumption is that a portion of these improvements can be incorporated into a satellite power plant design, such that the fuel cell and cooler specific weight can be reduced from 3.4 lbs/ft$^2$ to 1.0 lb/ft$^2$. In addition lighter weight composites are being developed for pressure vessels using ultra thin welded metal liners. If the performance loss in the fuel cell mode can be held to 50 mV below present performance and cell temperature increased to 300°F, a maximum specific energy density of 115 W-hrs/lb. is predicted.

- The dual function system holds the greatest potential for a high reliability module. This approach results in the need for the fewest number of cells, which, for a passive system, tends to substantially increase reliability.

## C. Technology Recommendations

- The regenerable fuel cell system, because of its high energy density and flexibility to operate in a number of potential orbits (high to low cycle life) warrants further technology development activities.

- Of particular interest is a "dual function" alkaline system which has the potential for very high energy densities. This is a completely passive design with the fewest number of cells per stack of all systems studied which could lead to high reliability and minimum system cost.

- To be successful in developing a dual function system requires that a major effort be directed at establishing a stable and high performance fuel cell cathode catalyst, which can also operate successfully in the electrolysis mode.

- Operation at high pressure (~1800 psia) is desireable because lightweight composite tankage and containment vessels can be used and in addition the higher pressure dramatically reduces the power plant specific volume.

- Operation at elevated temperature (300°F vs. 180°F) is also desireable, since the higher temperature increases fuel cell performance and thus tends to result in a reduced stack and containment vessel size and weight. Another viewpoint is that to establish a stable dual function cathode will in all likelihood result in a fuel cell performance lower than present cells. To ameliorate this effect the temperature can be increased. The higher temperature will also make heat rejection by means of radiation more effective and will result in an additional temperature can be increased. The higher temperature will also make heat rejection by means of radiation more effective and will result in an additional weight saving. To successfully construct a higher temperature cell will require a significant materials development program.

- Heat pipes are convenient means of carrying cell waste heat to the external heat rejection system. For this study flat plate heat pipes using water as the working fluid have been assumed and weights for off-the-shelf equipment have been used. Further studies should be conducted to optimize the heat pipe design for the specific heat fluxes and operating pressures of interest.

# II. INTRODUCTION

Future space satellite applications will require significantly higher power and energy density power systems than have been needed in the past. This report describes four high power $H_2$-$O_2$ fuel cell system concepts, which are designed to yield high energy density, high efficiency, and strive to eliminate failure prone components, so that the power system reliability is also high.

This report is divided into eight sections. Section I is a summary of the entire study and gives a brief description of each system, its advantages, the major results and conclusions and key recommendations. Section III is a generic description of all the systems and is intended to cover general areas common to each concept and also to explain differences in approach to certain functions for each system. Sections IV - VII cover each of the four system concepts in some detail with a schematic diagram, a description of components, a list of operating conditions and key assumptions, a summary of the major component weights, and a description of the fuel cell and electrolyzer stack and cell conceptual design, with material identified and approximate sizes defined. In the case of the dedicated and dual function alkaline systems, parametric studies were conducted to establish the sensitivity of energy density to specific design changes. Section VIII concludes the report with a general discussion of system reliability issues.

# III. GENERIC ENERGY STORAGE SYSTEM DESCRIPTION

## A. Description of System Concepts

Figure 1 shows the major components of a space satellite power system based on separate fuel cell and electrolysis components for energy storage. This system stores energy supplied by solar panels in the form of $H_2$ and $O_2$ gases obtained from the electrolysis of water. During this "recharge" period the solar panels supply all the power needs of the satellite system as well as the power for the electrolyzer. When the satellite is eclipsed, all the system power is obtained from fuel cells in the energy storage subsystem which consumes the stored $H_2$ and $O_2$, generating electricity and byproduct water. The overall energy storage cycle involves the following actions:

DURING THE DISCHARGE CYCLE (Solar eclipse periods)

- Transfer of $H_2$ and $O_2$ gases from tanks to the fuel cell stack
- Consumption of reactants in a fuel cell to generate power
- Removal of fuel cell product water
- Removal of fuel cell waste heat
- Supply of fuel cell power at a given voltage to the system bus
- Condensation and storage of product water
- Transfer of water to the electrolysis cell stack

DURING THE RECHARGE CYCLE

- Solar panels provide all the system power
- Bus power electrolyzes water generating $H_2$ and $O_2$ gases
- $H_2$ and $O_2$ gases are stored in external storage tanks
- Heat may be either added or removed from electrolyzer depending on operating conditions.

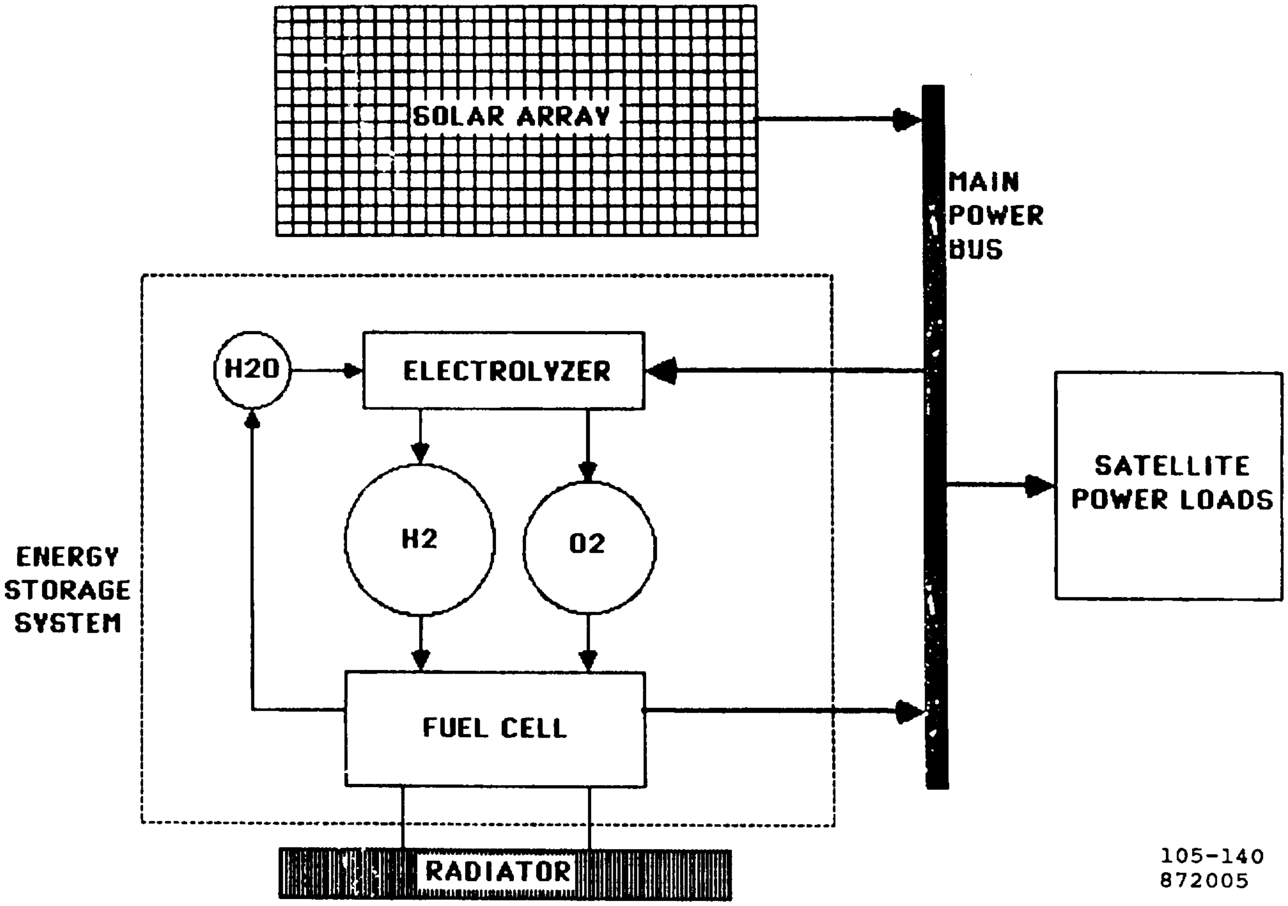

Figure 1. Satellite Energy Storage System

For this study it was assumed that these functions could be supplied by either of two system configurations; designated as dedicated or integrated cell stack systems. The type of cells studied in these two configurations used either alkaline or polymer membrane electrolytes. The dedicated systems consist of individual fuel cell and electrolysis cell stacks while the integrated system option assumes the fuel cell and electrolyzer cells are contained in a single stack, either as interleaved individual cells or as dual function single cells. Each system option presents unique problems and advantages when incorporated in an energy storage system but both must provide energy storage with high reliability by minimizing or eliminating moving parts such as pumps and blowers. Such systems will be referred to as "passive" or "static" in this report. The following sections describe both passive dedicated and integrated systems and how their designs uniquely meet requirements in three functional areas:

- Matching bus voltage levels
- Stack containment
- Cell stack water management

In addition the following functions common to both systems are discussed:

- Stack cooling
- Reactant storage and supply

## B. Matching Bus Voltage Levels

DEDICATED STACKS: The control of the power and voltage output of the stacks is simplified because the cell size and number of cells can be chosen independently for the fuel cell and electrolysis cell stacks. The number of cells per stack is chosen to be compatible with the specified 120 volt bus voltage and the cell area is set by the individual stack performance and the power requirements of each stack.

INTEGRATED STACKS: The integrated stack design may be composed of either interleaved separate fuel and electrolysis cells or a multiple number of bipolar single dual function cells. The interleaved cells are the same size and are placed back to back to minimize the distance required for the transfer of water between modes of operation. The total number of cells is chosen to meet the bus voltage requirement of 120 volts during fuel cell operation and the size of the cells is set by the performance and power requirements of fuel cell operation. The volts per cell required for electrolysis is a function of the required overall system efficiency, the system parasitic losses, and the chosen fuel cell stack volts per cell. A typical example of a 55% efficient system has a fuel cell volts per cell of .843 and the required electrolysis cell voltage of 1.5 resulting in a total stack voltage of a 120 volts in the fuel cell mode and 213 volts in the electrolysis mode. In order to more closely match the required 120 volt bus, the stack for the integrated option is split into two substacks and during fuel cell operation the substacks are connected in series outputting 120 volts. The substacks are then connected in parallel during the electrolysis mode of operation requiring an input voltage of 107 volts. Matching of the bus voltages and the required electrolysis stack voltages could be achieved in a number of ways; 1) by a relatively small adjustment in the bus voltages by a power conditioner added to the system, b) by fine tuning the fuel cell stack voltages, or c) by the use of more than two substacks in a more complex series-parallel arrangement.

## C. Stack Containment

DEDICATED STACKS: The fuel cell stack is run at relatively low pressure to permit the feeding of $H_2$ and $O_2$ from the higher pressure storage tanks without the use of compressors. The low pressure fuel cell requires no external containment vessel and can be designed in a similar fashion to Orbiter fuel cells which have rectangular stacks using internal o-ring seals to contain the reactant gases. On the other hand the electrolysis stack must be run at pressures up to the maximum pressure of the reactant storage tanks to permit filling of the tanks during the recharge period without the use of a compressor. The maximum operating pressure of the electrolysis stack is relatively high for the use of o-rings, therefore, in this study, the stack was assumed to be contained in a vessel.

INTEGRATED STACKS: This system contains both the fuel cells and electrolysis cells in a single stack and all the cells see the same operating conditions over the entire cycle of charge and discharge. Since the stack sees the full range of gas pressures, because the electrolysis cell must operate up to the maximum gas storage pressure and the fuel cell down to the minimum pressure, the integrated stack is contained in a pressure vessel.

## D. Cell Stack Water Management

DEDICATED STACKS: One problem, unique to the dedicated stack option, is the passive transfer of water over the relatively long distance from the fuel cell stack (where the water is formed during discharge) to the electrolysis cell stack (where the water is required during recharge). A number of passive water transfer options were considered including;

1. Diffusion of water vapor through $H_2$ and $O_2$ gas passages connecting the fuel cell and electrolyzer cell stacks.

2. Separation of pure water vapor in the fuel cell at low pressure, with subsequent condensation and external storage of the product water. Then prior to the recharge period employing one of the following options:

   a. Evaporation of the water with subsequent feed of the steam.

   b. An increase in water temperature with the resultant rise in pressure driving the liquid water directly into the electrolysis stack.

   c. Wick the liquid water directly into the electrolysis stack.

3. Separation of pure water vapor in the fuel cell at low pressure and then the transfer of the water vapor to an even lower pressure electrolysis cell stack where it is condensed and stored.

Option 1 is practical only for system arrangements where the pathlengths between the fuel cell and electrolyzer cells are short. Long water transfer paths would require large differences in the partial pressures of the water vapor in each cell stack, necessitating large differences in the cell operating temperatures or electrolyte concentration. This approach was considered impractical for this application.

Figure 2 shows a dedicated stack energy storage system with a stack water transfer system based on Option 2 described above. Both Options 2 and 3 assume the separation of a low pressure water vapor stream. This is accomplished by using a separator located in the anode passage of the fuel cell. It consists of a series of porous graphite plates filled with KOH/water in the alkaline systems or pure water in the PEM stacks. Each separator consists of a graphite fine pore plate sandwiched between two coarse pore plates also made of graphite. The coarse pore plates form the gas passages for the anode and pure water sides of the separator. In addition, these plates transfer current, provide physical support and store excess water to prevent the drying out of the fine pore. The central fine pore permits the transfer of water vapor from the medium pressure fuel cell anode gas passage to a relatively low pressure pure water vapor gas passage while preventing diffusion of $H_2$. The pore size of this plate is chosen to withstand the pressure differential between the anode and the water vapor passage. In Figure 2 a separate condenser is shown between the fuel cell and electrolyzer, and this water must be transferred to the electrolysis cell prior to the charge cycle by one of the three mechanisms described above. If there is no external condenser, the fuel cell product water vapor is transported directly to the electrolyzer where it is condensed and stored in porous graphite plates as mentioned in Option 3 above.

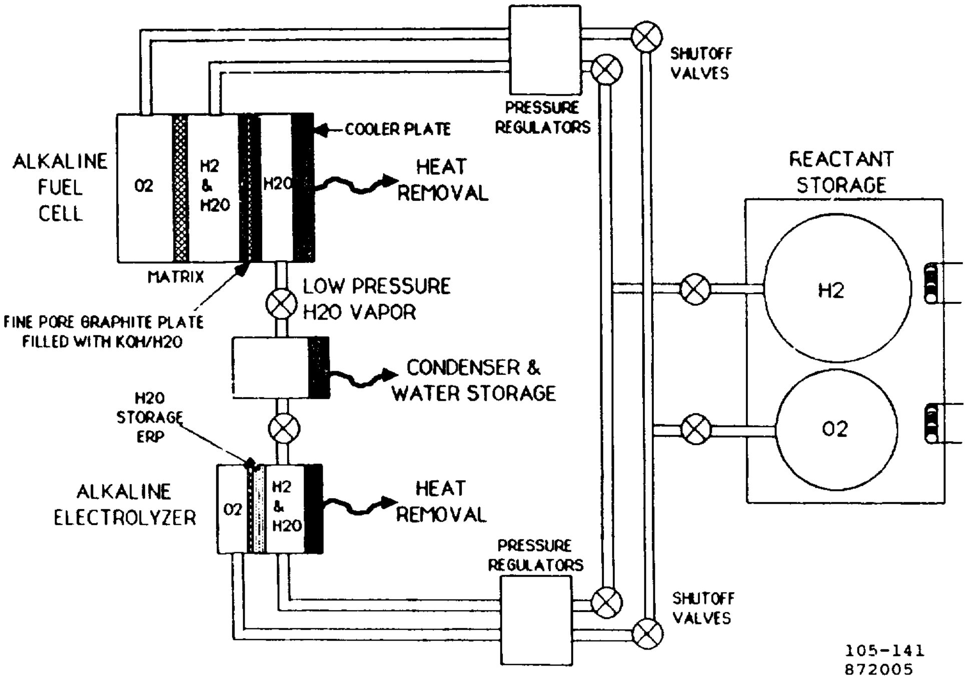

Figure 2. Dedicated Stack Energy Storage System
Static Water Transfer

INTEGRATED STACKS: The passive transfer of water from the fuel cell to the electrolyzer is relatively simple in the integrated system. The water is formed in the fuel cell mode and stored in a porous carbon electrolyte reservoir plate (ERP) adjacent to the fuel cell anode passage. The integrated system having interleaved cells has these water storage ERP's between alternate fuel cells and electrolysis cells and therefore water transfer is accomplished by the diffusion of water through the relatively short path length of the width of the ERP. Calculations have shown the diffusion of water through the liquid and vapor regions of the ERP can satisfy the water requirements for the electrolysis phase of operation in both a geosynchronous earth orbit (GEO) and Mid-earth orbit (MEO) application. The water transfer rates required in the GEO application for an integrated system is proportional to the electrolysis cell current density. The current density is relatively low due to the large electrolysis cells that result from the equal fuel cell and electrolysis cell areas imposed by the configuration, and is also low due to the short discharge period (1.2 hrs) relative to the charge period (22.8 hrs) characteristic of GEO. MEO consists of equal length charge and discharge periods of three hours. This does increase the required operating electrolysis mode current densities and the corresponding water transfer flow rates, however estimates show that the proposed integrated system configuration can meet the MEO requirements.

## E. Stack Cooling

DEDICATED OR INTEGRATED SYSTEMS: Several methods for passively cooling the cell stacks in the energy storage systems studied were identified. It was assumed for this study that waste heat would be transferred to the edge of the cell stacks or their containment vessels where it would be collected and subsequently rejected to space through a radiator system provided by the satellite thermal control systems. Thermal system weights for this study include only the necessary components to conduct the heat to the stack edge and do not include the satellite thermal system weights.

In the first approach waste heat is conducted to the edge of the stack by use of solid cooler plates located between every cell in the stack. These plates must be light weight, tolerant to the cell operating environment, and have a high thermal conductivity to minimize the temperature drop required to remove the cell waste heat. Two candidate materials were identified for use as cooler plates, graphite or gold plated magnesium. Graphite was selected as the baseline material for this study. The graphite cooler is designed to provide the following specific functions:

- Maintain an average cell temperature of 180°F.
- Limit the temperature drop across the cell active area to 20°F.
- Electrically isolate coolers from each other and the stack vessel.

The 180°F operating temperature with a 20°F variation in temperature across the cell is consistent with present operation of alkaline fuel cell systems. This insures good stack performance and operating lifetimes compatible with the GEO mission requirements emphasized in this study. All the near term fuel cell or electrolyzer systems studied, whether alkaline or PEM, operated between temperatures of 150 to 200°F. The cooler plate designs are based on providing adequate cooling for the fuel cell mode of operation since this represented the maximum heat rejection duty. The electrolysis cells were designed to operate at the thermal neutral potential, although means are provided to add or remove heat for off-design conditions. The configuration of the fuel cell stack has a significant impact on the weights of graphite coolers designed to meet the operating criteria of a 20°F temperature drop across the cell. Figure 3 shows the trend of the cell aspect ratio (cell length/cell width) on the specific weight of the coolers. A 55% efficient system using cells with an aspect ratio of 1 (square) would have heavy coolers due to the relatively thick plates dictated by long pathlength required for the removal of the cell waste heat and the limitation of a maximum cell temperature drop of 20°F. A cell aspect ratio of four gives the same cell active area with a heat removal pathlength only 1/4 as long as a square shaped cell resulting in a substantial reduction in the cooler weights. Rectangular and annular stack configurations both provide the large cell length to width ratios required by the graphite coolers. A rectangular shaped stack is possible for the dedicated systems where the fuel cells are run at 60 psia

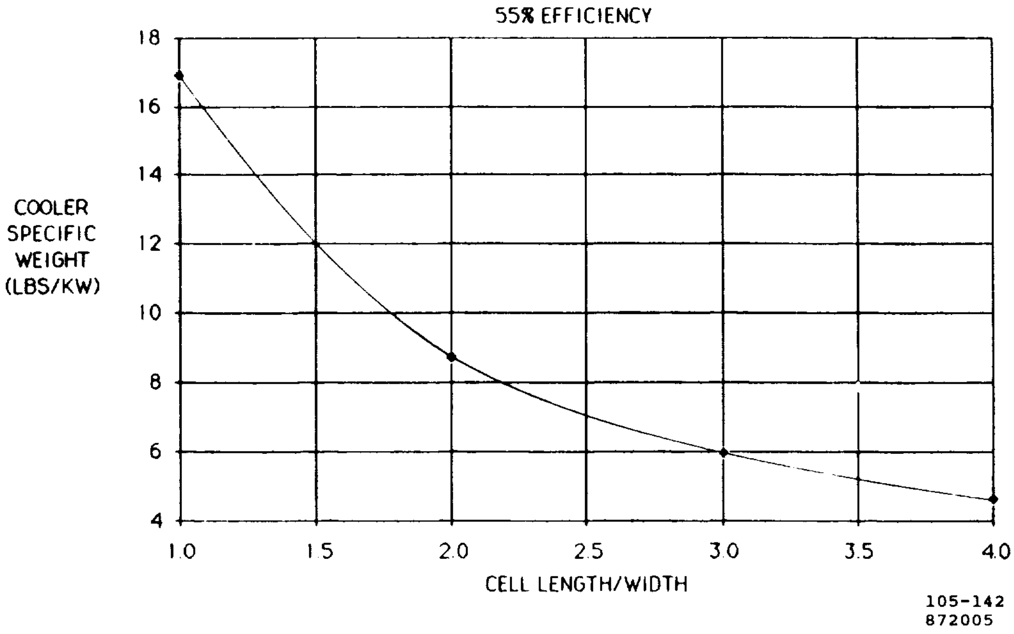

Figure 3. Graphite Cooler Weights vs Cell Aspect Ratio

or less and do not require pressure vessel containment. The integrated systems must have pressure vessels therefore the configuration chosen for these options was annular which permits relatively narrow cell stacks, results in a structurally preferable shape for the containment vessel, and is conducive to the close contact with the vessel wall required for heat removal.

A second cooling option involves the use of heat pipes in place of solid graphite coolers. Heat pipes consist of a wick and a working fluid, such as water (used for this study), enclosed in a thin metal shell (a flat plate design in this case). Heat from the cell active area boils the water inside the heat pipes pushing the vapor to the condenser section of the pipe. The heat pipe condenser is located at the edge of the stack which is cooled externally, condensing the water vapor, and subsequently returning the liquid water to the evaporator section of the heat pipe by the capillary action of the wicks. Heat pipe coolers can remove more heat than the graphite plates with the same overall temperature gradient and essentially isothermal operation across the width of the cell active area. Square and circular cell stack configurations are possible with heat pipe coolers, that were impossible with solid graphite coolers, due to their low cross cell temperature drop. A heat pipe cooler is heavier than a graphite cooler therefore it cannot be placed between every cell since this would result in a significant weight penalty. System weights can be kept low by using fewer heat pipe coolers per stack (more cells between coolers), which is possible due to their increased heat transfer capacity. The exact number of cells per cooler is determined by the assumed maximum temperature rise of 20°F between the heat pipe and the highest temperature cell and by the maximum cooling capacity for a given heat pipe design. For this system the cooler design was based on a flat heat pipe manufactured by NOREN PRODUCTS, INC. For this study the following characteristics were assumed:

Overall Size: 4" wide X 9" long X .125" thick
Weight with plated magnesium skin material: .53 lbs
Maximum Heat Removal Capacity: 280 watts

This heat pipe design was assumed to be adaptable to a circular or square configuration while maintaining the same specific specific weight (2.1 lbs/ft$^2$) and the same maximum heat capacity of 280 watts for the .125 inch thick heat pipes. A final design for a heat pipe cooler must address the problems of materials compatability in the cell operating environment, and the pressure capability of flat plate heat pipe designs to elevated stack operating pressures. This study was meant as a first pass analysis to determine the feasibility of using heat pipe coolers for these applications.

## F. Reactant Storage and Supply

DEDICATED OR INTEGRATED SYSTEMS: The reactant gases, $H_2$ and $O_2$, are generally stored in tanks external to the cell stacks. These reactants must be transferred to and from the storage tanks without the use of compressors and this is accomplished by maintaining an appropriate pressure differential between the tanks and the fuel cell or electrolysis cell stacks. The pressure difference provides the driving force for the required gas transport. The gases must be supplied to the fuel cell during its discharge, even as the tanks reach their minimum pressure, therefore the choice of fuel cell operating pressure and the required pressure difference for gas supply sets the minimum storage pressure. Similarly, the choice of the electrolysis cell pressure sets the storage tank pressure for both hydrogen and oxygen. Alkaline fuel cells used in space applications have typically operated at pressures of 60 psia or less, therefore, this was chosen as the minimum storage tank pressure. Similarly the best available information on near-term technology alkaline electrolysis cells showed they can supply reactants at a maximum pressure of 300 psia and this was assumed to be the maximum storage tank pressure. Higher operating pressures are possible and would result in weight savings for the energy storage system. The effects of higher operating pressures for electrolysis and storage was investigated for all the systems studied but this option should be considered a longer term prospect requiring a technology development effort.

The materials chosen for the construction of the reactant tankage must be compatible with the following requirements:

Temperatures: up to 180°F
Pressures of: 60 - 300 psia (Near term technology)
60 - 1800 psia (Advanced technology)
Life: 10 yrs (GEO)
5 yrs (MEO)
Cycles: 900 (GEO)
7300 (MEO)

These criteria can be met by the following metal tankage materials:

Inconel 718 for $H_2$ tankage
Cryoformed 301 stainless steel for $O_2$ tankage
Safety factor of 1.5

For this study all the systems operating at a maximum pressure of 300 psia were assumed to use the metal tankage described above. The higher pressure option (1800 psia) would require very heavy metal tankage and therefore, in keeping with advanced technology, lightweight composite materials were used. Composite tankage consists of thin walled metal liners (spherical or cylindrical) fully overwrapped with continuous high strength fibers embedded in resins. The resulting filament wound tanks are light and strong having typical design operating pressures of 1800 to 4500 psia. Early in the system studies it was assumed that composite tanks would offer a significant weight advantage relative to metal tanks even at low operating pressures (60 - 300 psia). Further study, including the contacting of a composite tankage manufacturer (Structural Composites Industries, Pomona, California) showed that composites have no weight advantage over metal tanks at 300 psia. Figure 4 summarizes the results of this investigation. At 300 psia the vendor quote for a composite tank holding 1.5 lbs of $H_2$ was 82 lbs compared to 60 to 80 lbs for metal tankage depending on the assumed safety factor (1.5 - 2.0). At 1800 psia the vendor quotes for composite tankage ranged between 12 to 22 lbs compared to metal tanks weighing 50 to 70 lbs. Composite tankage shows this weight advantage at high pressure because the thin metal liners with high strength overwraps are much lighter than the relatively thick walls of the metal tankage. This weight savings disappears at 300 psia as the wall thickness for the metal tanks approaches the thickness of the thin metal liner used for the composites. Manufacturing and structural limitations prevent the use of liners thin enough to extend the composite vessel weight advantage down to the 300 psia range. The transition between 300 and 1800 psia at which composites would be lighter than metal tankage could not be determined due to limited vendor data. The analysis of advanced technology systems using composite pressure vessels assumed an 1800 psia maximum operating pressure, lower pressures are possible but the weight gains for composite vs. metal tanks would be lower. Figure 4 implies that higher pressures would not significantly enhance the weight advantage of composites, and would require that the electrolysis cell operate at less favorable conditions.

Other functions that are provided by the reactant storage system include pressure regulation, tank temperature control, and shut off valves to isolate tankage from the fuel cell or electrolyzer depending on the mode of operation. Temperature control is vital since the stored reactants contain a small amount of water vapor and if the temperature drops too low the water will condense and be trapped in the reactant tankage. This would reduce the energy storage capability of the system.

Therefore, heat losses should be minimized by insulating the tanks and any reduction, caused by depressurizing the tanks must be countered by use of a small electric heater, or through use of waste heat from other sources.

In the case of the integrated systems, the pressure vessel surrounding the cell stack can be used to store some, or all, of the reactant gases. The amount of gases that can be kept directly inside the stack pressure vessel is a function of the system operating pressure range the size of the stack pressure vessel itself. A larger vessel is required for the annular cell stack design using solid cooler plates than is needed for the relatively compact circular disk stack configuration which uses heat pipe coolers. Either configuration could store all the reactant gases if the operating pressure were raised to a high enough level. The first pressure plateau for an annular design is at an efficiency of 55%. At this pressure all the $H_2$ and $O_2$ can be stored internally requiring no external pressure vessels and therefore no pressure vessel penetrations to supply the reactant gases. In the case of the more compact designs (e.g. heat pipe cooled circular stacks) a much higher pressure would be required to achieve the same integrated reactant gas storage.

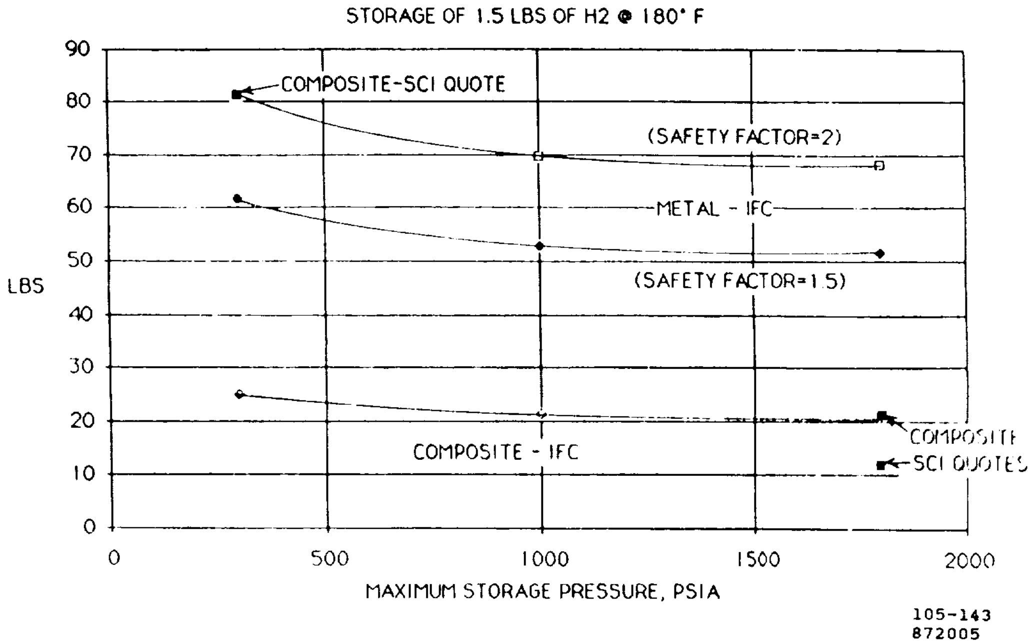

Figure 4. Composite vs All Metal Reactant Gas Tankage

## IV. INTEGRATED ALKALINE SYSTEM

### A. Description of System Concept

A passive, integrated, $H_2$-$O_2$ alkaline fuel cell/electrolyzer concept was selected as the initial configuration for both the MEO and GEO designs. The proposed system utilizes completely passive techniques for regenerative fuel cell operation and control, to provide improved reliability over state-of-the art systems which employ a number of dynamic components, such as pumps, blowers, separators, and valves to properly maintain operation of the system.

The basic fuel cell module for this concept consists of a hydrogen tank, an oxygen tank, and an integrated fuel cell - electrolyzer cell stack (Figure 5). The stack utilizes annular fuel cell and electrolysis cells alternately stacked inside of a pressure vessel, as shown in Figure 6. Water is stored within porous electrolyte reservoirs within the stack. Passive water transport is achieved by diffusion from the fuel cell to the electrolysis cell. During discharge, product water from the fuel cell reaction is stored in porous carbon reservoir plates. Waste heat is conducted to a graphite plate located between cell pairs and then conducted through the plane of the plate to the pressure vessel wall. This heat may be rejected from the vessel wall by a circulating coolant loop or by heat pipes attached to the circumference of the wall with their condensing sections attached to a space radiator or heat storage reservoir. During charge, (electrolysis operation) the water reactant is transferred from the porous carbon reservoir of the fuel cell by liquid and vapor diffusion to a porous plate in the electrolysis cell assembly.

Current is collected at the cell edges and transferred by metallic pins located around the periphery of the plastic inner and outer cell frames. The atmosphere inside the pressure vessel is hydrogen which is connected directly to a hydrogen storage tank. Oxygen is fed and collected through manifolds molded into the inside edge frames of the annular cells and is connected to a separate oxygen storage tank (Figure 6).

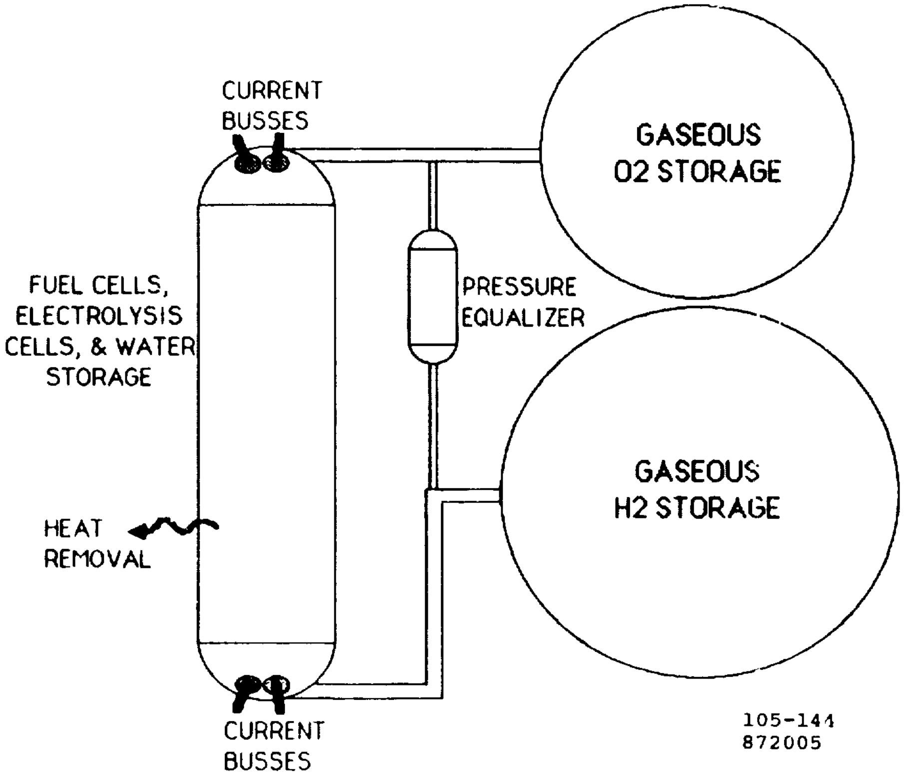

Figure 5. Basic Module for Passive, Integrated H2 - O2 Alkaline Regenerative Fuel Cell

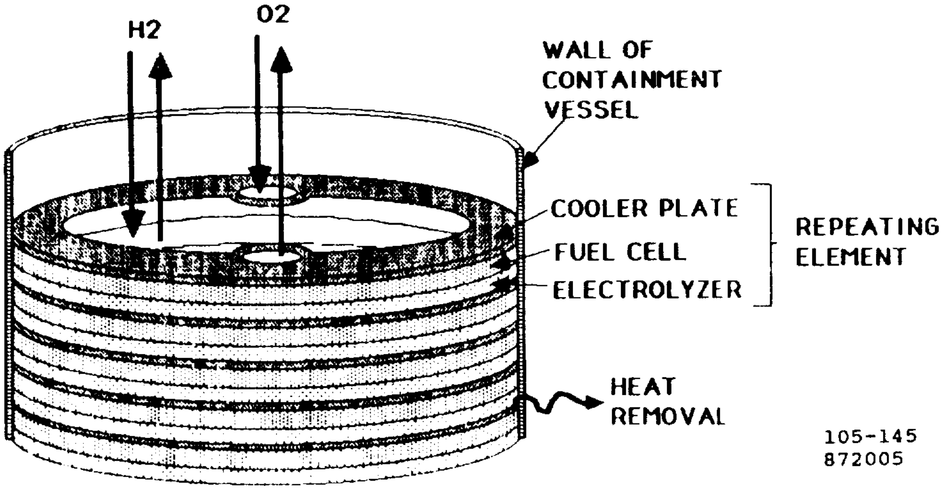

Figure 6. Cell Stack Cutaway Sketch

The system is launched in the charged mode, with hydrogen and oxygen stored in the reactant tanks at full pressure, approximately 300 psia. Bootstrap startup is accomplished in a matter of minutes by feeding hydrogen and oxygen to the fuel cells. The waste heat generated by inefficiencies within the cell, plus heat supplied by electrical heaters fed from the fuel cell output, are used to raise the cell stack to operating temperature. During startup, heat rejection from the pressure vessel wall should be inhibited to minimize start-up time. The inner wall temperature of the cell stack pressure vessel and the reactant tanks are maintained above 156°F to prevent water condensation.

During normal discharge operation reactant pressure decreases from 300 psia to 60 psia, and electrolyte concentration in the fuel cell decreases from 45 to 32 percent KOH. If the reactant tanks tend to cool, waste heat from the fuel cell thermal management system may be used to maintain tank temperatures, or electric heaters may be used for this purpose, at some loss in efficiency.

Hydrogen loss due to diffusion through the reactant tank wall was estimated to be small (less than .1 percent of the hydrogen consumed over a ten year period). The low diffusion rate is attributed to the relatively low operating temperature and pressure in the tank. A bellows or equivalent device is included in the system to insure that the differential pressure between reactants is maintained within the allowable limits for the cells during the entire deployment period of the satellite.

## B. Operating Conditions and Assumptions

The technology assumptions and major design conditions used for this study are listed in Figure 7.

The fuel cell performance and life estimates are based on data from operation of the Orbiter fuel cell power plant and from testing of the NASA-Lewis advanced fuel cell configurations at UTC. Similar data for the electrolysis cell is based on information reported by LSI under contract NAS3-21287.

The operating temperature of 180°F and maximum operating pressure of 300 psia were chosen primarily because they are within the regime of operating experience, and allow existing models of performance and cell life to be reliably used. To date a fuel cell stack has demonstrated 18,000 hours of operation, while an electrolysis cell has run for over 30,000 hours, both in a cyclic mode. Analysis indicates that the primary wear-out mode of a fuel cell is the excessive conversion of the alkaline electrolyte from hydroxide to carbonate. In the proposed regenerative closed system, no carbonaceous gases will enter the cell from external reactants. Only the degradation of stack materials will cause carbonation. Using the materials presently being tested in fuel cells, a projected life of 150,000 hours is estimated before individual cell wear out occurs.

While the efficiency goal for the MEO orbit was 55 percent, analysis indicated that designing to this level would cause excessively high current densities when the power plant was operating at peak conditions (50 kW). This limit necessitated designing for a relatively low current density of 100 ASF at the average power point (18 kW), which results in an overall higher system efficiency (61.3%), at some reduction in the specific energy density.

The total system is composed of three separate modules. Each module is capable of delivering one half maximum power and contains its own reactant supply system. During normal operation two modules will be operating and one kept in cold standby condition. The standby module will allow continuation of full operational capability in the event of a single point failure in the power system.

| | MEO | GEO |
|---|---|---|
| • MAX. OPERATING PRESSURE, PSIA | 300 ⟶ | ⟶ |
| • MIN. OPERATING PRESSURE, PSIA | 60 ⟶ | ⟶ |
| • NOMINAL OPERATING TEMP., °F | 180 ⟶ | ⟶ |
| • PERFORMANCE BASIS | ORBITER & LSI DATA ⟶ | ⟶ |
| • EFFICIENCY @ AVG. POWER, % | 61.3 | 55.0 |
| • PARASITE POWER, (% OF AVG. POWER) | | |
| FUEL CELL | 1.5 ⟶ | ⟶ |
| ELECTROLYSIS | .7 ⟶ | ⟶ |
| • LIFE, YRS (WEAR-OUT MODE) | ~ 17 ⟶ | ⟶ |
| • POWER PLANT ARRANGEMENT | • 2 X 25 kW Modules<br>• 1 Spare 25 kW Module | • 2 X 12.5 kW Modules<br>• 1 Spare 12.5 kW Module |
| • NO. OF REACTANT TANK PAIRS PER MODULE | 1 ⟶ | ⟶ |
| • NO. OF CELL STACKS PER MODULE | 2 ⟶ | ⟶ |

105-146
872005

Figure 7. Design Conditions and Assumptions

## C. Weight and Volume Summary

A weight and volume summary for each of the satellite applications is shown in Figure 8. As can be seen, the cell stack weights represent over 62 percent of the total. This fact points out the importance of developing lightweight, corrosion resistant materials of construction and also of increasing cell performance. Higher operating pressure, and temperature are studied in section H.

The fuel cell weight is about a factor of three heavier than the electrolysis cells because the product water is stored in the fuel cell portion of the stack, and the vast majority of waste heat is generated in and must be removed from the fuel cell. If the graphite cooler plates could be eliminated, and the waste heat carried to the pressure vessel wall by the remaining fuel cell elements, a weight reduction of about 10 percent could be effected, which would increase the specific energy density by about the same amount and would shorten the cell stack length by 17 percent. This design approach merits study for future work.

As indicated, a miscellaneous weight value of 10 percent was included to account for piping, support structure, bellows, electric heaters, and current take-offs which were not specifically designed during this study.

The module equipment volume tabulated in Figure 8 represents the volume of all equipment but does not account for a packaging factor which will depend on layout and weight distribution requirements for the satellite.

Figures 9 and 10 give overall dimensions for the major module equipment for MEO and GEO orbits. Optimization for the size and number of reactant tanks, again, must depend on launch limitations and specific satellite requirements.

## WEIGHT AND VOLUME SUMMARY
## SINGLE MODULE

| | MEO | GEO |
|---|---|---|
| • Module Rating, kW | | |
| Max. | 25.0 | 12.5 |
| Avg. | 9.2 | 12.5 |
| • Fuel Cells, Electrolysis Cells, and Water Storage, Lbs | 479 | 235 |
| • Stack Containment Vessels, Lbs | 43 | 26 |
| • Stored Hydrogen, Lbs | 3.1 | 1.9 |
| • Hydrogen Tankage, Lbs | 96 | 52 |
| • Stored Oxygen, Lbs | 24.6 | 15 |
| • Oxygen Tankage, Lbs | 49 | 30.0 |
| • Miscellaneous | 77 | 46.8 |
| • Total Weight, Lbs | 771 | 407 |
| • Specific Energy Density, W-Hrs/Lb | 35.7 | 36.9 |
| • Total Module Equipment Volume, $Ft^3$ | 61 | |

Figure 8.

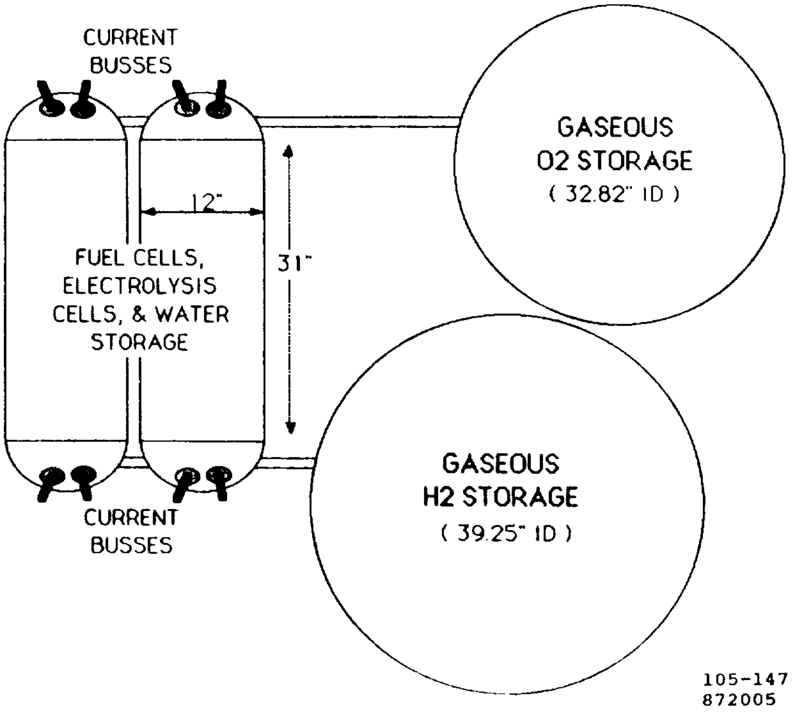

Figure 9. 25 kW Module for Energy Storage Mid Earth Orbit

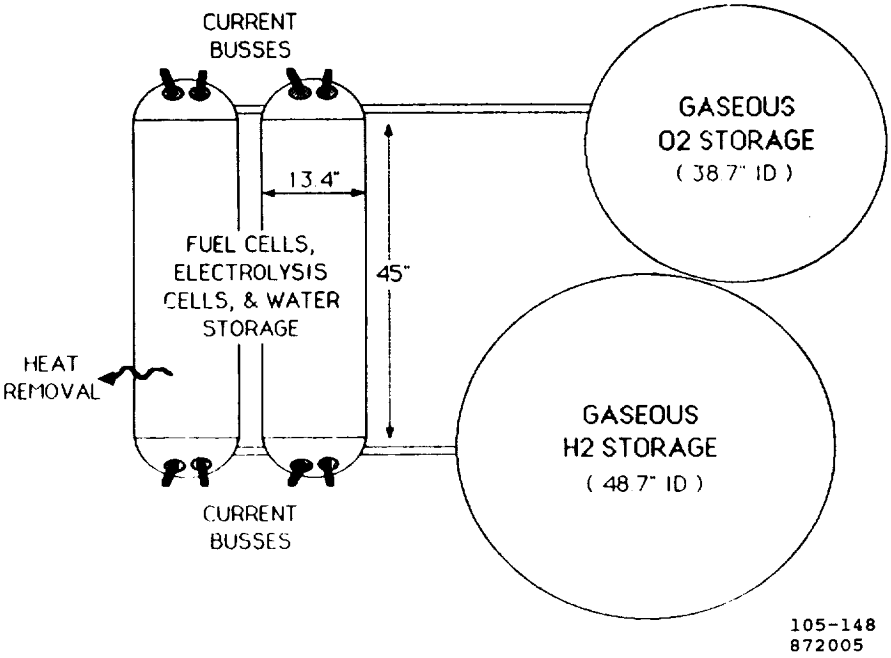

Figure 10. 12.5 kW Module for Energy Storage Geosynchronous Earth Orbit

## D. Cell Stack Summary

Data relating to both fuel cell and electrolyzer cell stack performance and physical configuration are given in Figure 11.

For MEO, the system plant must be designed to deliver a maximum power of 2.7 times the design average value. To accomplish this without excessive heat generation and water production, the fuel cell operates at a relatively low current density at average power. For the point design selected, a current density of 100 ASF was chosen, yielding a value of 323 ASF at peak power. Subsequent parametric studies, discussed later in this report, indicate that a 10 percent increase in specific energy density would be achieved if 150 ASF had been chosen for the design point. This, however, would have resulted in 3.5 point decrease in efficiency.

| | MEO | GEO |
|---|---|---|
| • STACK EOL* GROSS PEAK POWER RATING (kW) | 12.7 | 6.34 |
| • FUEL CELL EOL AVG POWER CELL VOLTAGE | .94 | .84 |
| • EOL PEAK POWER CELL VOLTAGE | .79 | N/A |
| • FUEL CELL AVERAGE CURRENT DENSITY, ASF | 100 | 340 |
| • PEAK CURRENT DENSITY, ASF | 323 | N/A |
| • ELECTROLYZER EOL CELL VOLTAGE | 1.5 | 1.5 |
| • ELECTROLYZER CURRENT DENSITY, ASF | 100 | 18 |
| • CELL AREA, $FT^2$ | .52 | .31 |
| • NO. OF FUEL CELLS PER STACK | 96 | 71 |
| • NO. OF ELECTROLYSIS CELLS PER STACK | 96 | 71 |
| • TOTAL STACK HEIGHT, IN. | 45 | 31 |
| • INSIDE DIAM. OF STACK, IN. | 7.8 | 8.2 |
| • OUTSIDE DIAM OF STACK, IN. | 13.3 | 12.1 |
| • PRESSURE VESSEL MATERIAL | INCONEL 718 ——→ | |
| • PRESSURE VESSEL THICKNESS, IN. | .030 | .027 |
| • HEAT REJECTION | CONDUCTION TO VESSEL WALL | |
| • CURRENT COLLECTION | TO METAL PINS IN EDGE FRAME | |

*EOL - END OF DESIGN LIFE

105-149
872005

Figure 11. Cell Stack Summary

For GEO, a high design current density was selected for the fuel cell to minimize hardware weight. For this application a constant power level was assumed. Charge time for the electrolysis cells is relatively long, 22.8 hours. This results in a low power requirement for charging, but since the electrolysis cells have the same active area as the fuel cells they can operate at very low current density. Significant resistance losses are allowed in the design of the electrolysis cells to generate sufficient waste heat to maintain the stacks at operating temperature during the long charge period.

The cell stacks are placed in a pressure vessel in which the atmosphere is hydrogen, thus no hydrogen manifolding is required. Oxygen, however, is manifolded through the inner plastic frame area of the cells (see Figure 6). The oxygen manifolds and the oxygen compartments in the cell stack must be separated from the hydrogen by elastomer seals. The pressure differential between the two gases is slight, with the oxygen pressure being designed to be slightly above the hydrogen. Any leakage of oxygen into the hydrogen gas will be converted to water on the electrode catalyst and recycled into the system.

Figure 12 is a cutaway view of a single cell repeating element for the MEO cell stack. Each element includes a fuel cell, an electrolysis cell and a graphite cooling plate. The total thickness of each cooler plate/fuel cell/electrolyzer assembly is .47 inches, with the majority of this space taken up by porous carbon plate which contain electrolyte and stored water. The heat, generated primarily during the discharge mode, is conducted to the cooler plate and then along the plane of the plate to the pressure vessel wall. The cooler plate is electrically insulated from the cell stack by thin Teflon sheets. The maximum temperature differential between the vessel outer wall and the hottest point in the cell is 35°F at the peak discharge power condition. Figure 13 shows a similar cutaway view of a single cell repeating element for the GEO application.

ORIGINAL PAGE IS
OF POOR QUALITY

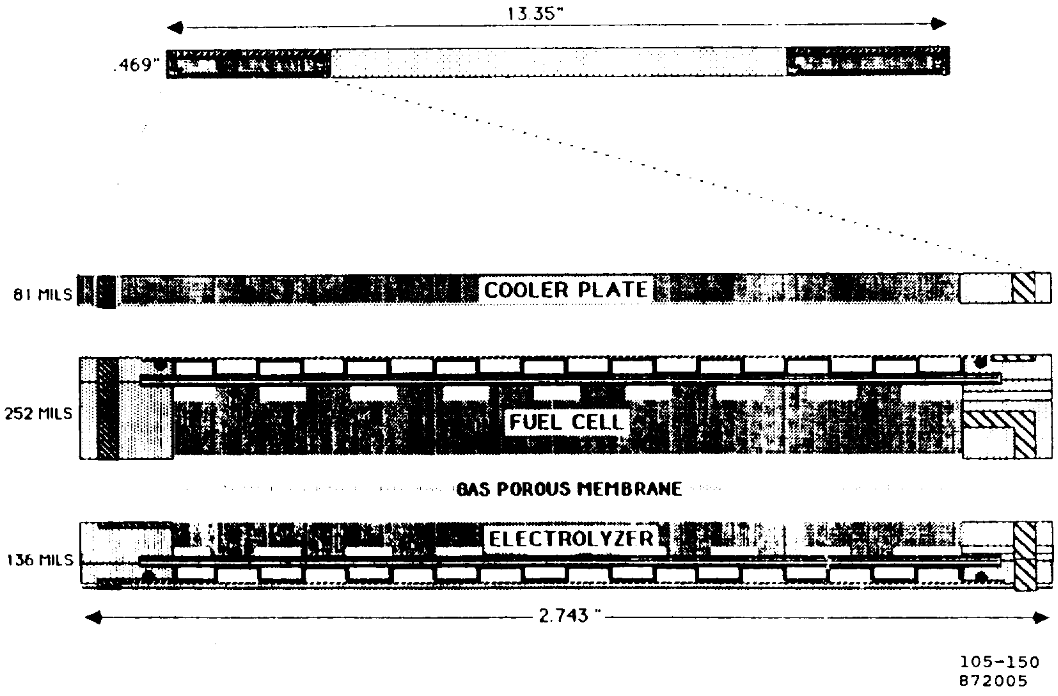

Figure 12. 25 kW MEO System Repeating Cell Element

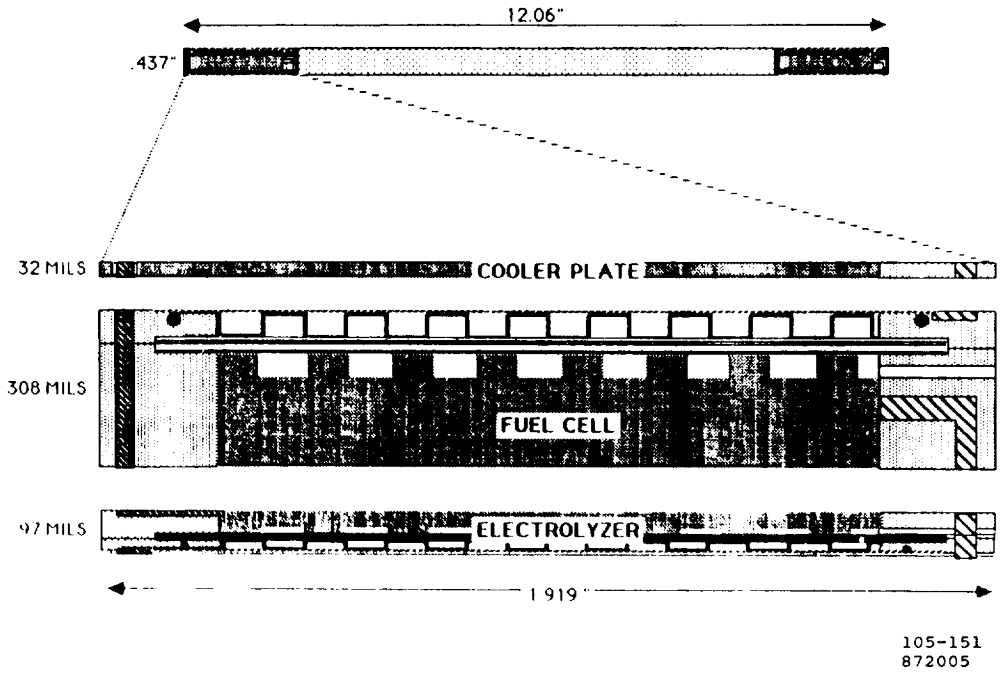

Figure 13. 12.5 kW GEO System Repeating Cell Element

During the charge (electrolysis) mode, water must diffuse through the porous carbon plates containing electrolyte and across a hydrogen gas barrier separating the fuel cell from the electrolysis cell. Calculations have been made to show that the rate of water diffusion can easily support the design current levels in the electrolysis cell.

Current is conducted to the edge of the cells and transferred, in series, to the adjacent cells by means of metallic pins located in the plastic edge frames and spaced around the periphery of the cells. The fuel cell current transfer is through the inner frame, while that for the electrolysis cell is in the outer frame. A number of alternate current transfer arrangements were conceived during the study, and could be incorporated without significantly affecting the overall weight.

## E. Voltage Characteristics

Anticipated dc voltage characteristics delivered from the fuel cell and required by the electrolysis cell are shown in Figure 14. Fuel cell performance was assumed to vary due to pressure and electrolyte changes in accordance with a UTC developed cell model. The decay rate of .3 microvolts per hour per 100 ASF is based on slow but gradual loss of anode and cathode performance with time as well as electrolyte carbonation. As indicated in the LSI report conducted for NASA (NAS3-21287 Sept. 1984) the effect of pressure on electrolysis performance is small. Also, based on the long term results of LSI pulsed cell tests, decay is considered negligible.

As shown in Figure 14, the maximum voltage change at average discharge power for the MEO application is 17 volts (from 197 volts at the beginning of life to 180 volts at the end of life). The voltage change at peak power is somewhat greater, varying between 178 and 152 volts. Assuming that each of the two electrolysis stacks in a module are connected in parallel, the required input voltage would be 144 volts.

For the GEO mission, the discharge voltage varies from 137 to 120 volts. The charge voltage is estimated at 107 volts.

Figure 15 shows the fuel cell performance (current density vs volt/cell) for four key points of the GEO system operation:

| OPERATING POINT | PSIA | %KOH | HRS LIFE |
|---|---|---|---|
| 1. Beginning of Discharge | 300 | 45 | 500 |
| 2. Beginning of Discharge | 300 | 45 | 40,000 |
| 3. End of Discharge | 60 | 32 | 500 |
| 4. End of Discharge | 60 | 32 | 40,000 |

**ASSUMPTIONS**

| | |
|---|---|
| FUEL CELL | • PERFORMANCE VARIES DUE TO PRESSURE & CONCENTRATION CHANGES<br>• DECAY = 0.3$\mu$V/HR/100ASF |
| ELECTROLYZER | • PERFORMANCE INDEPENDENT OF PRESSURE & CONCENTRATION CHANGES<br>• DECAY~ NEGLIGIBLE |
| CONFIGURATION | • F/C STACKS IN SERIES<br>• E/C STACKS IN PARALLEL |

| RESULTS | MEO | GEO |
|---|---|---|
| F/C DISCHARGE, 300 PSI BOL*, VOLTS | 197 (178**) | 137 |
| F/C DISCHARGE, 60 PSI BOL, VOLTS | 183 | 126 |
| F/C DISCHARGE, 300 PSI EOL*, VOLTS | 195 | 131 |
| F/C DISCHARGE, 60 PSI EOL, VOLTS | 180 (152**) | 120 |
| E/C CHARGE, VOLTS | 144 | 107 |

*BOL = BEGINNING OF LIFE, EOL = END OF DESIGN LIFE
**F/C VOLTAGE AT PEAK POWER

105-152
872005

Figure 14. Voltage Characteristics vs. Life and Charge/Discharge Cycle

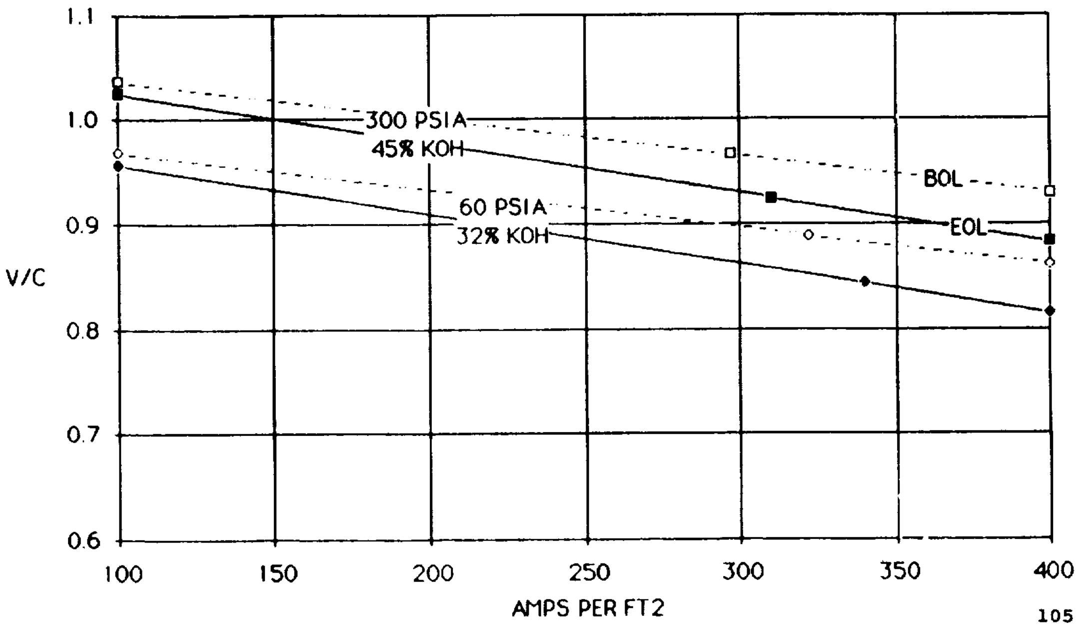

105-153
872005

Figure 15. Alkaline Fuel Cell Performance

## F. Heat Rejection Characteristics

A graphite cooler plate is located between each cell and serves to conduct waste heat to the pressure vessel wall. In order to insure a high level of performance, the design was based on a maximum 20°F temperature variation along the active portion of the fuel cell. This criteria essentially set the thickness of the graphite plate. A larger temperature variation would allow a thinner plate at the expense of lower cell performance. This is an area which is further studied in Section H.

Figure 16 shows the maximum rate of heat rejection and the maximum heat flux required to be removed from the pressure vessel surface for both the MEO and GEO application. For the MEO case, the heat rejection was calculated at the peak power point. At the conditions described in Figure 16, the outside wall temperature is 155°F for MEO and 148°F for GEO.

When power is reduced, the fuel cell average temperature would tend to drop at lower loads if the vessel wall temperature is held constant such as would occur if variable conductance heat pipes are used for cooling. If the vessel wall temperature can be varied, such as might occur if a liquid coolant is used, the fuel cell temperatures could be maintained constant over a wide load range. In any case, since the system is cyclic in nature, it is quite possible that steady-state thermal conditions may never be completely achieved (except during the long GEO charge mode).

ASSUMPTIONS

- GRAPHITE PLATE LOCATED BETWEEN CELL PAIRS CONDUCTS WASTE HEAT TO PRESSURE VESSEL WALL.
- MAXIMUM CALCULATED $\Delta$ T SEEN BY F/C IS 20°F AT PEAK POWER POINT.

| RESULTS (PEAK POWER VALUES) | MEO | GEO |
|---|---|---|
| • PEAK POWER OF MODULE, kW | 25 | 12.5 |
| • HEAT REJECTION PER MODULE, BTU/HR | 76,100 | 33,366 |
| • HEAT FLUX AT PRESSURE VESSEL WALL, BTU/HR-FT$^2$ | 2,900 | 2,040 |
| • PRESSURE VESSEL OUTSIDE WALL TEMPERATURE, °F | 155 | 148 |

105-154
872005

Figure 16. Heat Rejection Characteristics

## G. Reactant Tankage Description

All metal vessel construction has been assumed for both the hydrogen and oxygen reactant tanks. As shown in Figure 17 for the hydrogen tank, Inconel 718 is assumed as the vessel material, while 301 stainless is used for oxygen. The choice of all metal tankage over composite tankage for the case of a 300 maximum system operating pressure is discussed in Section III.

Calculations to determine the diffusion of hydrogen through the Inconel metal wall indicated a loss of less than 0.1 percent of the hydrogen consumed over a ten year period. This analysis was based on limited data. However, the relatively low operating pressure range (300 to 60 psia) and low operating temperature (180°F) would indicate that low levels of loss may be expected.

REACTANT TANKAGE DESCRIPTION

| | MEO | GEO |
|---|---|---|
| Hydrogen Tank | Inconel 718 | |
| Hydrogen Tank Diam. In. | 48.7 | 39.3 |
| Hydrogen Tank Weight, Lbs** | 96 | 51.7 |
| Oxygen Tank* | Cryoformed 301 Stainless Steel | |
| Oxygen Tank Diameter, In. | 38.7 | 32.8 |
| Oxygen Tank Weight, Lbs** | 49 | 30 |

*Designed for maximum operating pressure of 300 psia and temperature of 180°F.

**Weights include 1 inch of insulation (gold metalized kapton film layers separated by borosilicate matt)

Figure 17

## H. Parametric Studies for the Integrated Alkaline System

To evaluate the impact of key assumptions and variables on the specific energy density, a number of parametric studies were conducted. These are listed below and discussed in the following paragraphs.

1 Energy Density vs. Module Rating (GEO)

2 Energy Density vs. Efficiency (GEO & MEO)

3 Energy Density vs. Cooler plate thickness and temperature drop (GEO)

4 Energy Density vs. Electrolyte Reservoir Plate (ERP) thickness (GEO)

5 Energy Density vs. Pressure (GEO)

6 Energy Density vs. Temperature (GEO)

### I. Effect of Module Power Rating

The NASA design requirements for GEO application is 25 kW. This could be achieved in one 25 kW module or with a number of smaller modules. The baseline case uses two 12.5 kW modules. Figure 18 shows the impact of varying the module size on system specific energy density. The figure indicates an increase of about 4% in energy density when going from a 25 kW module to two 12.5 kW modules. However, reducing the module size further does not result in a benefit. The improvement in energy density for smaller module sizes is due, primarily, to the weight savings associated with the stack containment vessel and the reactant gas pressure vessels. The lower power modules have smaller diameter vessels, requiring thinner walls and resulting in less weight per kW-hr of energy storage. For this study a minimum wall thickness of 20 mils was assumed to be the lower limit for fabrication. This limit is reached just below the 12.5 kW module size, which explains why there is no further energy density improvement below this size.

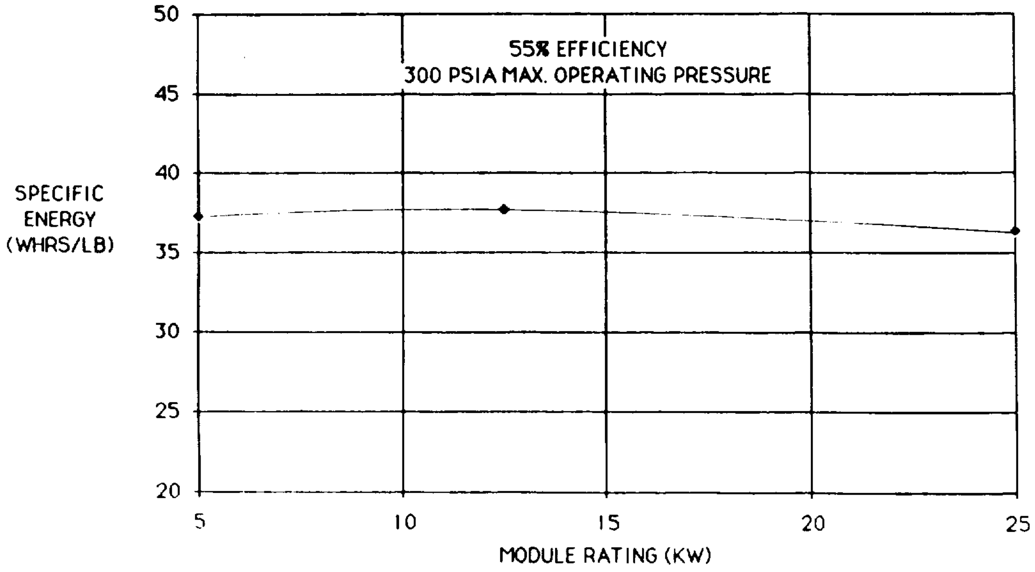

105-155
872005

Figure 18. Effect of Module Power Rating

J. Effect of Efficiency

A parametric analysis was conducted describing the variation of the system specific energy density as a function of efficiency. The results of this study are shown in Figure 19 for both the MEO and GEO applications.

It can be seen that the selection of 55 percent efficiency for GEO applications does not result in the highest energy density system. A 50 percent efficient system has a 6 percent higher energy density (40.1 Whrs/lb) than the 55 percent case (37.7 Whrs/lb). In the MEO application selecting an efficiency lower than 61.3 percent used in the point design would also yield a higher energy density with a maximum value approaching 38 Whrs/lb. This lower efficiency case however has very high peak power current densities and the more conservative design point was chosen for the base case.

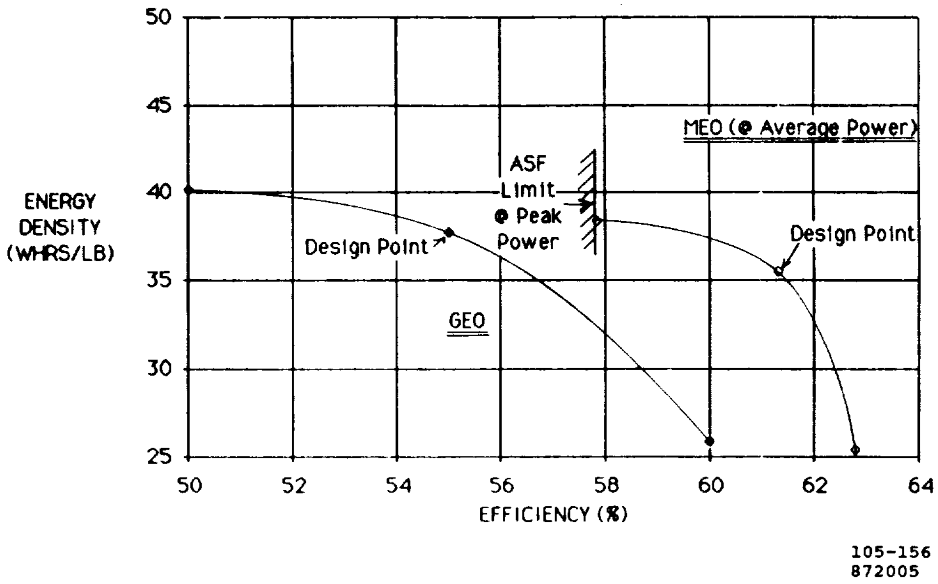

Figure 19. Impact of Efficiency on Specific Energy Density

## K. Effect of Cooler Thickness

Varying the thickness of the cooler plate changes the temperature drop required across the fuel cell for heat removal. This temperature drop was varied from 10 to 60°F by changing the thickness of the cooler plate while maintaining an average cell temperature of 180°F. Since the average temperature was unchanged it was assumed that the fuel cell performance was constant. The results of this parametric analysis, shown in Figure 20 indicates relatively small impact on the overall system weight over a large change in cooler thickness and associated cooler temperature drops. The reference case assumes a 20°F temperature drop with a cooler thickness of .032-inches. The 20°F delta T is consistent with assumptions made for alkaline fuel cell performance based on the advanced Orbiter powerplant. There seems to be no incentive to increase the delta T since even a 60°F drop reduces the system weight less than four percent.

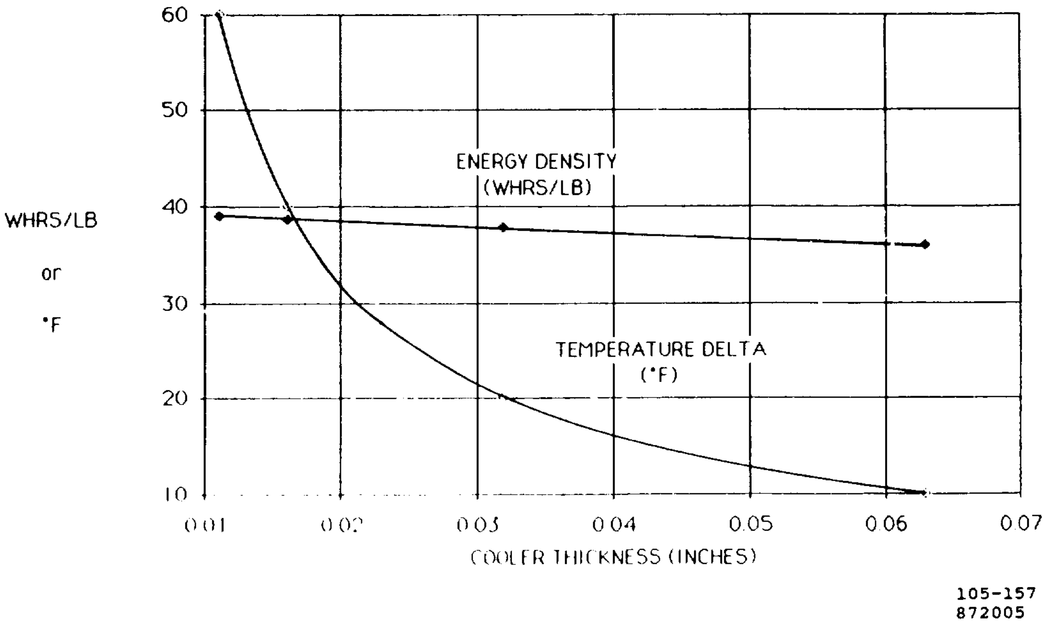

Figure 20. Effect of Cooler Thickness

## L. Effect of ERP Thickness

Figure 21 shows the effect of varying the fuel cell ERP thickness on the energy density of the storage system module. Water produced during fuel cell discharge is stored in the ERP and its total volume must remain relatively constant. A thinner ERP would have to be wider, implying a wider fuel cell active area. A thinner ERP would have the following impacts on component weights:

THINNER ERP AND WIDER CELL YIELDS:

> HEAVIER COOLER PLATES thickened to maintain a constant 20°F temperature drop across the wider cell.
>
> HEAVIER CELLS due to lower fuel cell performance caused by the higher edge current collection losses of a wider cell.
>
> LIGHTER EDGE SEALS due to a decrease in the overall stack height. The ERP thickness decreases faster than the required increase in the cell cooler thickness to maintain a 20°F temperature drop across the cell.

As shown in Figure 21 the net weight does not significantly change for a wide variation in the ERP thickness. This is a result of the cooler plate and cell weight changes being cancelled by the opposite change in the edge seal weights.

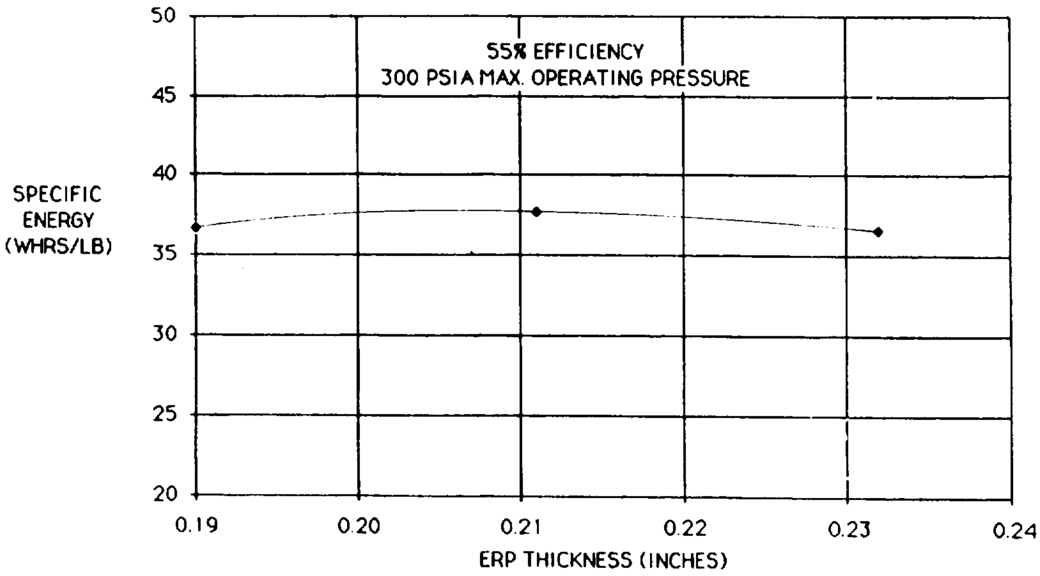

105-158
872005

Figure 21. Effect of Fuel Cell ERP Thickness

## M. Effect of Pressure

As discussed in Section III, the benefit of high pressure operation on system weights comes from the significant advantage of composite versus all metal construction for reactant and stack containment tankage. Figure 22 shows that operating the system at a maximum pressure of 1800 psia and using composite materials for all pressure vessels results in a significant weight advantage over the 300 psia baseline system which uses all metal construction. Higher pressure also significantly reduces the energy storage system volume. Figure 23 shows an 1800 psia system option resulting in 1/5 the volume of the 300 psia system.

From Figure 22 it can be seen that at a system efficiency of 55%, all the reactant hydrogen can be stored within the fuel cell containment vessel. At an efficiency of 60% both reactants can be stored within the containment vessel, thus not only eliminating the reactant tankage volume, but also, the complexity associated with feeding the reactants to the fuel cell and the structural penetrations required.

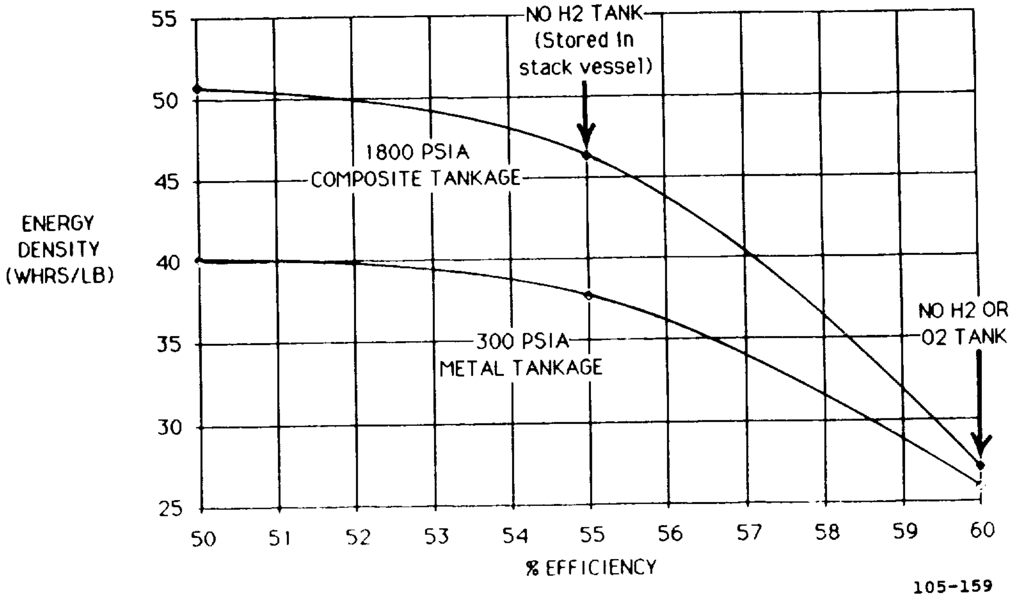

105-159
872005

Figure 22. Effect of Pressure on Energy Density Variable Efficiency

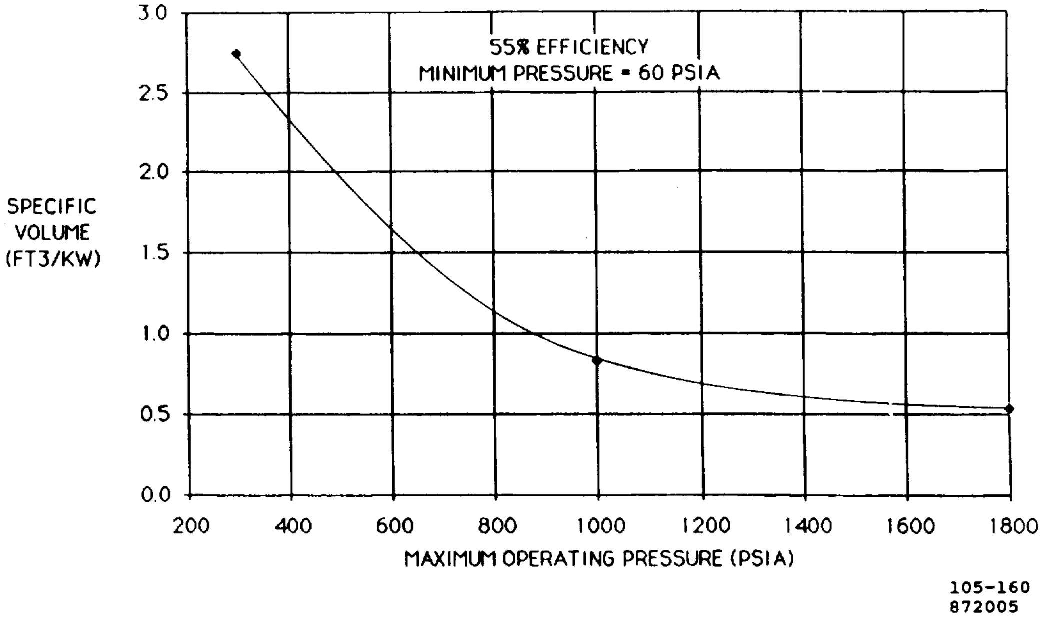

Figure 23. System Volume vs Maximum Operating Pressure

## N. Effect of Temperature

Figure 24 shows the effect of cell stack temperature on the energy density for the GEO application. Significant improvements in the system's energy density may be possible if the fuel cell operating temperatures could be raised from the baseline condition of 180°F to 300°F or higher. The temperature effect is shown for both a 300 psia maximum operating pressure using metal reactant gas tankage and for an 1800 psia case with composite tankage. The combination of composite materials and relatively high cell temperature could result in system energy densities greater than 60 Whrs/lb.

The temperature correction of the fuel cell performance is based on extrapolation of experimental data and further tests would be required to verify the performance. Other concerns requiring further study include the effect of changes in the water vapor pressures above the electrolyte at higher temperatures and its impact on stack performance, water storage, and water transfer to the electrolysis stack.

The major activity would be the development of materials which will be compatible in the higher temperature cell environment and will provide consistent performance over the required life of the power plant.

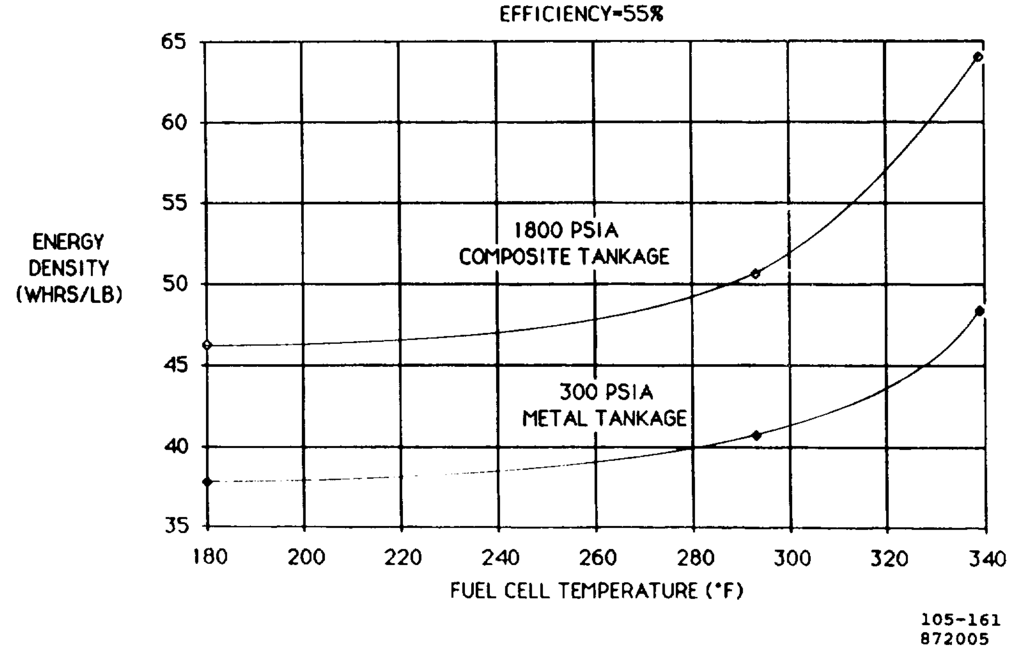

Figure 24. Effect of Temperature on Energy Density

## V. DEDICATED ALKALINE SYSTEM FOR GEO APPLICATION

### A. Description of System Concept

A passive, dedicated, $H_2$ and $O_2$ alkaline regenerative system concept was studied for the GEO satellite application. The basic module for this concept is shown in Figure 25 and consists of both hydrogen and oxygen storage tanks, and alkaline fuel cell stack, a separate alkaline electrolysis cell stack enclosed in a pressure vessel, and an external condenser. The module is designed to provide 12.5 kW net power output at an overall energy storage efficiency of 55%. Two modules would be used to provide the 25 kW total power output.

During the discharge period $H_2$ and $O_2$ reactant gases are fed from pressurized storage tanks through pressure regulators to a relatively low pressure fuel cell.

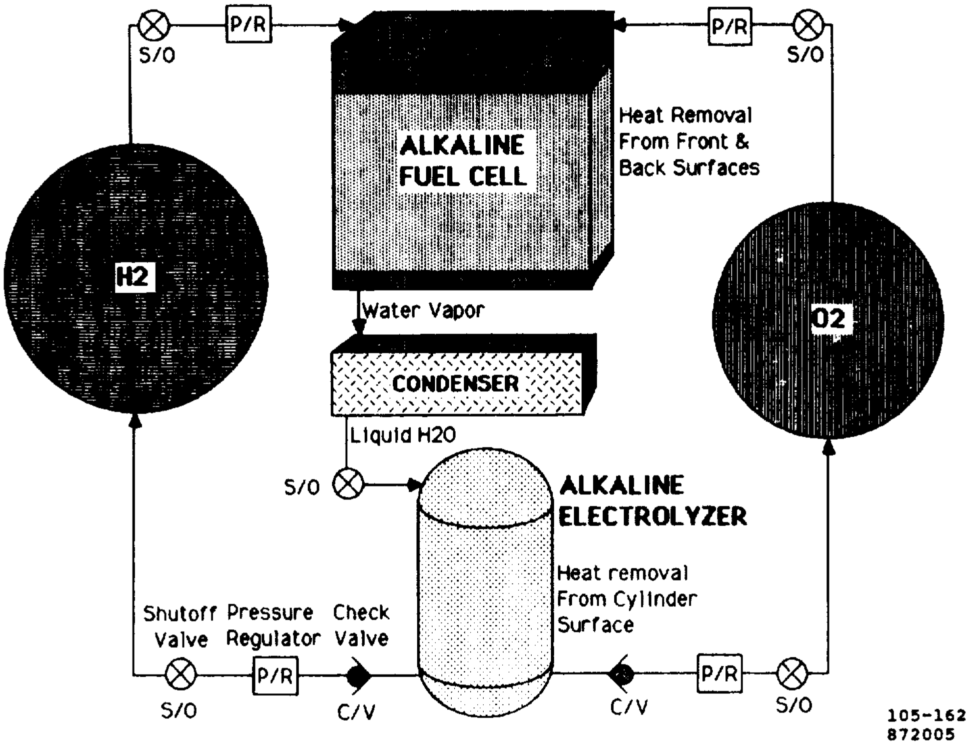

Figure 25. Dedicated Alkaline Energy Storage System

The pressure of the fuel cell was fixed by the choice of the static water removal method described in Section III. It involves the separation of water vapor from the anode gas passage across a fine pore graphite plate to a low pressure water vapor manifold. The pure water vapor pressure in this manifold is a function of the cell temperature and the concentration of the electrolyte in the fine pore separator plate. The cell stack operating pressure would be the sum of the equilibrium water vapor pressure of this manifold plus the amount of cross cell pressure differential that the fine pore plate can maintain. The low pressure stream of pure water vapor leaving the fuel cell is fed to a heat exchanger and is condensed and the resultant liquid water is fed to the electrolysis cell stack where it is stored in a porous graphite Electrolyte Reservoir Plate (ERP). The use of an external condenser, in place of condensing the water directly inside the electrolysis cell stack, removes the requirement for significant heat removal (heat of condensation) through the wall of the pressure vessel surrounding the electrolysis cell stack.

The water stored in the electrolysis stack is converted, during the recharge period, to $H_2$ and $O_2$ gases by power supplied by the satellite power bus. During the recharge period the electrolysis stack is isolated from the reactant storage tanks by a series of shut-off valves. This allows the evolving reactant gases to increase the stack pressure until it reaches its design value. At this point regulating valves maintain this pressure while feeding gases into the storage tanks. When the tanks are fully charged the electrolysis stack is again isolated by shutoff valves and the stack is run in a fuel cell mode until most of the remaining $H_2$ and $O_2$ gases within the reactant passages are consumed. This lowers the stack pressure and makes it ready to receive the low pressure water stream from the condenser during the discharge period.

## B. System Operating Conditions and Assumptions

The previous section described the general system operating concept while this section is meant to document the exact operating conditions and assumptions chosen for the system used in the final weight analysis.

Fuel cell system:

- Rectangular stack with no pressure vessel
- Graphite coolers with 20°F cross cell temperature rise
- 12.5 kW net power output per module
- Alkaline electrolyte - 32% KOH, 68% water
- 180°F operating temperature
- 16 psia operating pressure
- 4.3 psia pressure of separated water vapor stream
- 1.5% parasite power requirements

Electrolysis cell:

- Circular stack contained in a metal pressure vessel
- Graphite coolers with 20°F cross cell temperature rise
- 1.2 kW gross power input per module for GEO application
- Alkaline electrolyte - 32% KOH, 68% water
- 170°F operating temperature
- 300 or 1800 psia maximum operating pressure
- 2 to 3 psia pressure during fuel cell discharge period
- .7% parasite power requirements

Reactant Tankage:

- Minimum storage pressure of 60 psia
- Metal construction for maximum pressures of 300 psia
- Composite tankage for maximum pressures of 1800 psia

The fuel cell was operated at .84 V/C and 295 ASF. This performance was based on an advanced Orbiter alkaline powerplant with the cell voltage reduced by 45 millivolts to correct for the lower operating pressure of this system (16 psia vs. 60 psia for Orbiter). The alkaline electrolysis cell voltage was fixed at 1.5 volts per cell and 75 ASF. At this potential almost no waste heat is generated, eliminating the need for elaborate stack cooling during its operation. The use of an external condenser also eliminates the need for the electrolysis cell coolers to be sized for removal of the heat of condensation of the water stored in the ERP's. The ERP does, however, impose a limit on the maximum electrolysis current density due to the relatively slow rate at which water diffuses through the electrolyte to the reaction site at the electrode. Using a pump to supply water to the electrolyzer would allow higher operating current densities, but would require a high pressure pump, involving parasite power and incorporating rotating equipment which will affect system reliability. The water supply method used in this system option is passive, eliminating the pump by condensing and transferring the water into the ERP at low pressure, and later diffusing it to the surface of the electrolysis cell during high pressure operation.

## C. System Weight Summary

Figure 26 shows the weight breakdown for a 12.5 kW module dedicated, alkaline energy storage system module operating at 55% efficiency for both low (300 psia) and high (1800 psia) pressure electrolysis operation. The weight breakdown shows that the 1800 psia option is significantly lighter, due primarily to the use of composite materials for the reactant storage tanks. A more detailed description of the high and low pressure tankage is given in Section III of this report.

For the other system components the following assumptions were made in determining their weights. The fuel cell and electrolysis cell as well as stack non-repeat parts, such as endplates, were scaled from data available for an advanced Orbiter fuel cell design. The solid graphite coolers, required in both stacks, were sized to provide the required 20°F maximum cross cell temperature difference, and a porous graphite plate was sized for product water storage in the electrolysis cell stack. The condenser was scaled based on a design used in the Orbiter powerplant. A miscellaneous weight, equal to 10% of the sum of the basic component weights, was included to account for piping, support structure, electric heaters, insulation, and other small components.

12.5 KW NET POWER OUTPUT PER MODULE
55% WHR EFFICIENCY
GRAPHITE PLATE COOLERS

| | 300 PSIA METAL TANKAGE | 1800 PSIA COMPOSITE TANKAGE |
|---|---|---|
| FUEL CELL STACK | 132 | 132 |
| ELECTROLYSIS CELL STACK | 75 | 75 |
| H2 & TANKAGE | 60 | 21 |
| O2 & TANKAGE | 44 | 22 |
| EXTERNAL CONDENSER | 14 | 14 |
| PRESSURE REGULATORS & VALVES | 14 | 14 |
| MISCELLANEOUS | 38 | 31 |
| **TOTAL LBS** | 377 | 309 |
| **WHRS/LB** | 39.8 | 48.6 |

105-153
872005

Figure 26. Dedicated Alkaline Energy Storage Systems Module Weight Breakdown

## D. Cell Stack Summary

Figure 27 shows the fuel cell stack for the dedicated alkaline system. It is rectangularly shaped to facilitate heat removal by graphite cooler plates located between every cell. It is modeled after the alkaline Orbiter fuel cell in that it is a low pressure, rectangularly shaped stack using internal o-ring seals not requiring an external pressure vessel. During fuel cell operation gases are manifolded through passages located in the edge seals. These gases include $H_2$ and $O_2$ being fed to the cells, and water vapor which is being removed and transferred to the electrolysis cell stack. This stack employs bipolar current collection with the stack current flowing directly through the cells, water separators, and cooler plates to current collectors at either end of the fuel cell stack. Bipolar current collection does require that the cooler plates, which extend to the outside edge of the stack, be electrically isolated from each other to prevent shorting out cells. This can be achieved by use of an elastomeric compound applied to the edge of the cooler plates. The compound is electrically non-conductive but has relatively good thermal conductivity.

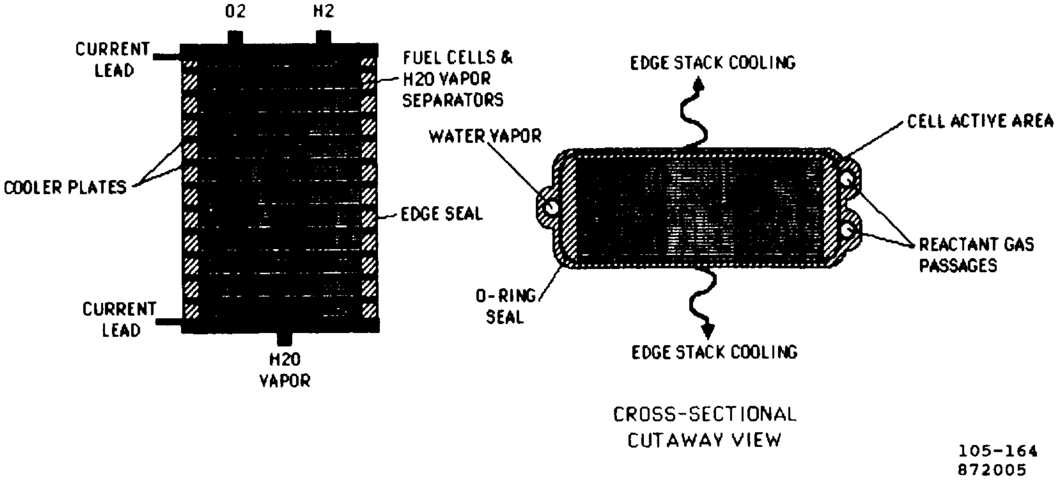

Figure 27. Alkaline Fuel Cell Stack

The internal detail of a single repeating element for the dedicated alkaline fuel cell system is shown in Figure 28. It shows that the anode of gas passages/ERP and the water separation plates are made of graphite while the cathode gas passage is made of formed nickel sheet with a monel cover plate to be compatible in an oxidizing environment. The water separator shown in Figure 28 consists of two graphite ERP's placed back to back separated by a thin fine pore of graphite. The plate and the ERP's are filled with the same KOH/water electrolyte mixture found in

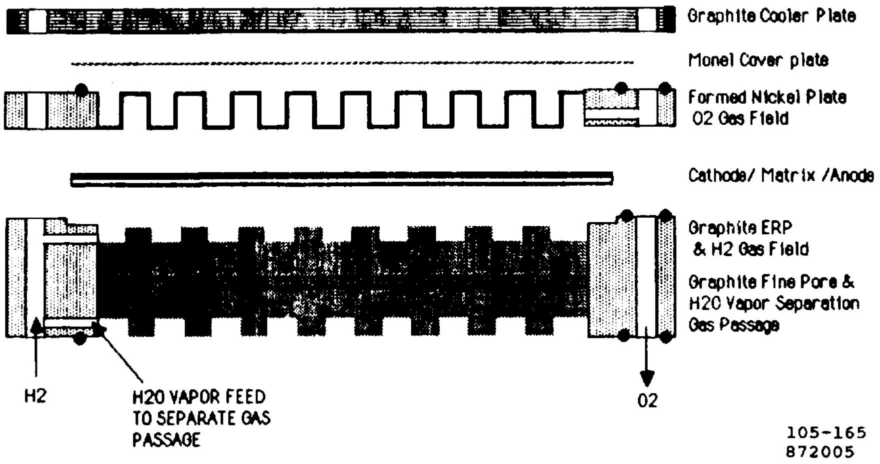

Figure 28. Alkaline Fuel Cell Repeating Element

the rest of the cell. The fine pore plate is chosen to have an average pore diameter sufficient to maintain the pressure differential between the moderate pressure anode gases (16 psia) and the low pressure pure water vapor compartment (4.3 psia). The fine pore passes pure water and prevents the diffusion of diluent $H_2$ gas. The ERP's on either side of the fine pore provide physical support, a path for current collection, and a reservoir to keep the fine pore plate filled with electrolyte during pressure transients. The ERP's in the fuel cell stack do not have to store the product water since it is actively removed as it is formed, therefore the ERP's are designed for the minimum thicknesses consistent with structural and manufacturing considerations.

Figure 29 shows a cutaway drawing of the alkaline electrolysis cell stack. This stack operates at high pressure (up to 1800 psia) and requires a pressure vessel. The circular electrolysis stack configuration is possible, even with the use of graphite cooler plates, because the heat rejection requirements are very low due to the product water being condensed externally and the cell being operated close to its thermo-neutral potential. Any waste heat is carried from the cells by graphite cooler plates to the edge of the cell stack and then through the pressure vessel wall to an external cooling system. Heat pipe cooling and the direct transfer of product water vapor from the fuel cell to the electrolyzer are options which were not studied for this system but are considered for the dedicated SPE system discussed in Section VI.

A cross section of the electrolysis cell repeating element is shown in Figure 30. Its major difference from the fuel cell element is the incorporation of a large porous graphite ERP on the $H_2$ side for storage of the product water transferred from the fuel cell. The cell stack is still a bipolar current collection arrangement with gas manifolding located in the stack edge seal area. This stack does not require a separate manifold for the water since it is fed directly into the hydrogen gas passages where it is stored in the ERP.

Figure 31 summarizes the fuel cell and electrolysis cell stack configurations for a 55% efficient, 12.5 kW dedicated alkaline stack module designed for a GEO satellite application.

ORIGINAL PAGE IS
OF POOR QUALITY

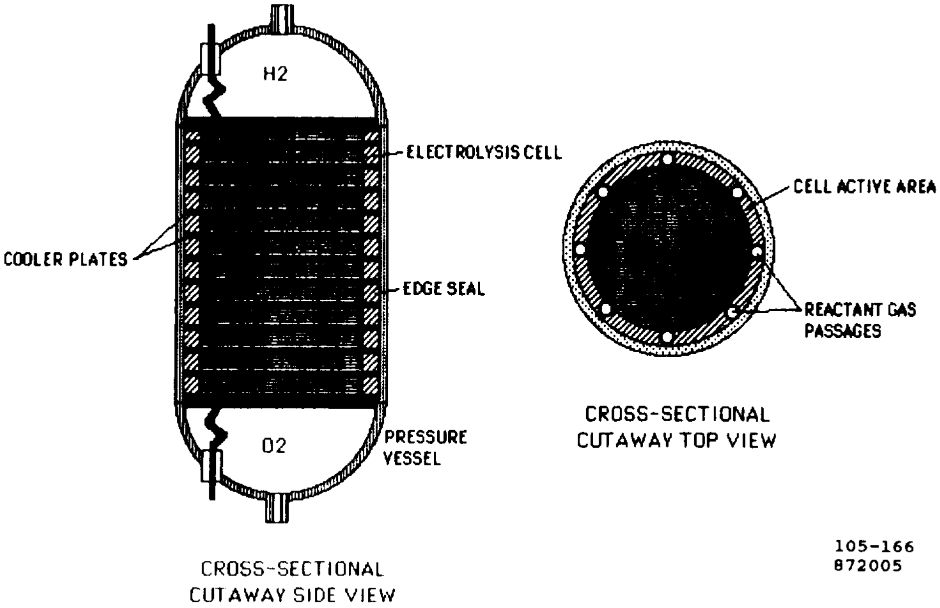

Figure 29. Alkaline Electrolysis Cell Stack

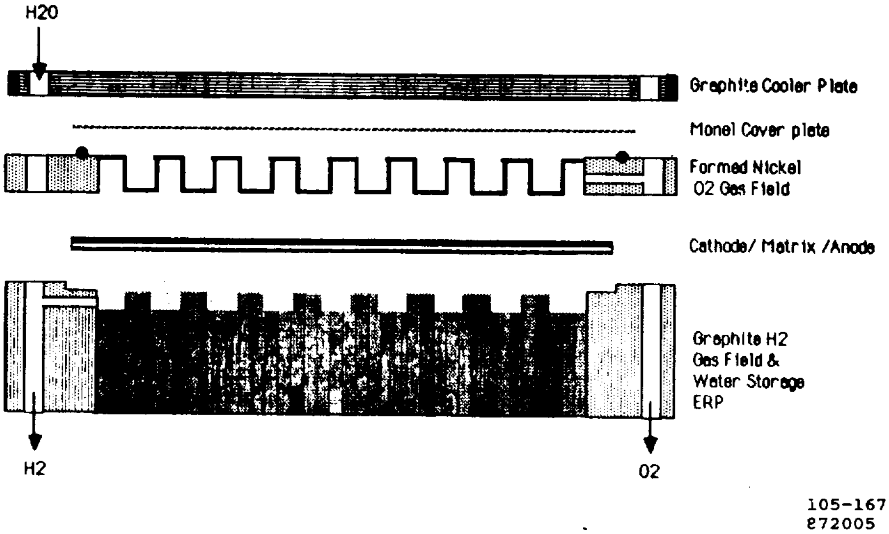

Figure 30. Alkaline Electrolyzer Repeating Element

**FUEL CELL STACK:**

12.5 NET POWER OUTPUT (END OF LIFE)
120 VOLTS PER STACK
.843 VOLTS PER CELL
295 AMPS PER FT2
.359 FT2 PER CELL
142 CELLS PER STACK
CELL LENGTH = 15.7 INCHES (INCLUDES EDGE SEAL)
CELL WIDTH = 3.9 INCHES (INCLUDES EDGE SEAL)
STACK HEIGHT = 50 INCHES (INCLUDES END PLATES)
GRAPHITE COOLER PLATES EVERY CELL
BIPOLAR CURRENT COLLECTION

**ELECTROLYSIS STACK :**

1.2 GROSS POWER INPUT (END OF LIFE)
33 VOLTS PER STACK
1.5 VOLTS PER CELL
75 AMPS PER FT2
.5 FT2 PER CELL
22 CELLS PER STACK
CELL DIAMETER = 10.1 INCHES (INCLUDES EDGE SEAL)
STACK HEIGHT = 22 INCHES (INCLUDES END PLATES)
GRAPHITE COOLER PLATES EVERY CELL
BIPOLAR CURRENT COLLECTION

105-168
872005

Figure 31. Dedicated Alkaline Cell Stack Summary

# VI. DEDICATED POLYMER MEMBRANE ELECTROLYTE SYSTEM

## A. Description of System Concept

A passive, dedicated, $H_2$ and $O_2$ polymer membrane electrolyte (PEM) fuel cell/electrolyzer concept was studied for a GEO point design. The basic module for this concept is shown in Figure 32 and consists of a hydrogen tank, an oxygen tank, a PEM fuel cell stack, and a PEM electrolysis cell stack enclosed in a pressure vessel. The module is designed to provide 12.5 kW net power output at an overall energy storage efficiency of 55%. This concept is identical in many respects to the dedicated alkaline system studied in Section V. The major differences between the systems being in the absolute cell stack performance levels, the impact of diffusional loses of reactants through the SPE membranes, and material changes to be compatible with PEM.

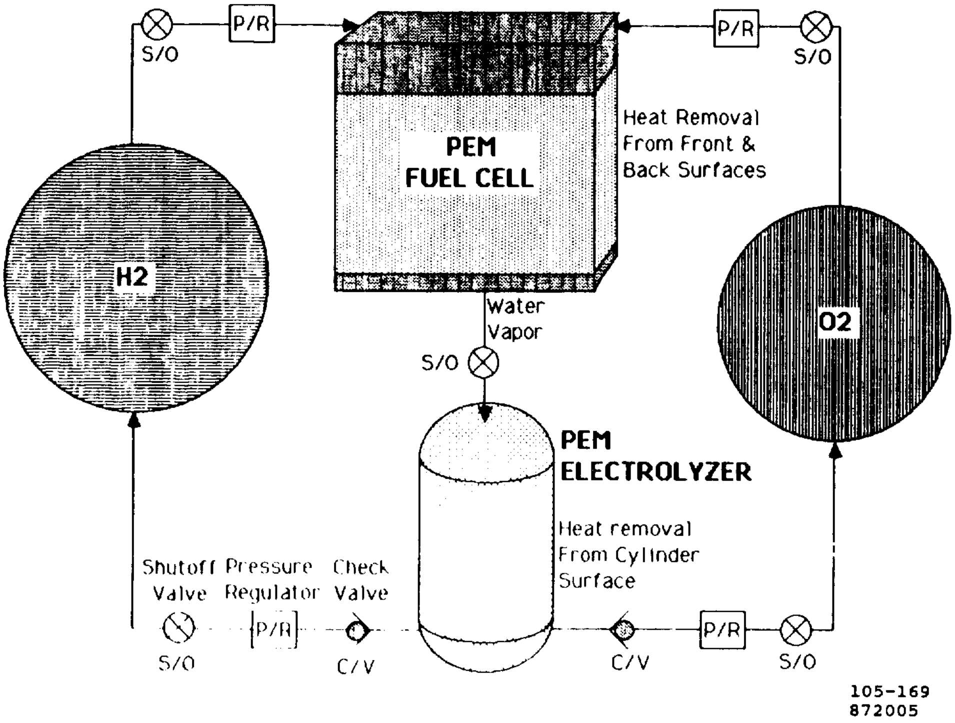

Figure 32. Dedicated PEM Energy Storage System

During the discharge period $H_2$ and $O_2$ reactant gases are fed from pressurized storage tanks through pressure regulators to a relatively low pressure fuel cell. The operating pressure of the fuel cell was selected at 30 psia to be compatible with proven PEM technology and because significant performance data was available at this condition. Product water liquid formed in the fuel cell cathode is collected from the electrode surface through the wicking action of coarse and fine pore graphite plates. These plates separate the cathode gas passage and the water vapor manifold. The equilibrium water vapor pressure in a pure water manifold is higher than the equivalent pressure in the alkaline system. This requires a pressure differential of 18 psia to be maintained across the separator plates. If further studies show that this pressure differential cannot be maintained then the PEM cell stacks could be run at a lower pressure with only a small loss in performance. A low pressure stream of pure water vapor is separated in the fuel cell and fed to an even lower pressure electrolysis cell stack where it is cooled, condensed and stored in a porous graphite Electrolyte Reservoir Plate (ERP).

During the recharge period, power is fed to the electrolysis cell stack where a two step process occurs. First, the cell is run as an oxygen concentrator transferring $O_2$, which has diffused into both anode and cathode passages during its dormant period, back into the anode passage. Secondly, the power converts the water stored in the electrolyzer ERP, to $H_2$ and $O_2$ gases increasing the electrolyzer stack pressure to its design level and then continuing at this level in recharging the empty reactant gas storage tanks. When the tanks are fully charged shut off valves isolate the electrolysis stack and the stack is run in a fuel cell mode for a short time until the $H_2$ and $O_2$ gases remaining in the stack are consumed. This lowers the electrolysis stack pressure and prepares it to receive the low pressure water vapor stream from the fuel cell stack during the discharge period.

## B. System Operating Conditions and Assumptions

This section describes the operating conditions and assumptions chosen for the system used in the final weight analysis. The general system parameters included:

Fuel cell system:

- Rectangular stack with no pressure vessel
- 12.5 kW net power output per module
- 120 volts
- Polymer Membrane Electrolyte (9 mil thick membranes)
- 200°F operating temperature
- 30 psia operating pressure
- 11.5 psia pressure of separated water vapor stream
- 1.5% parasite power requirements

Electrolysis cell:

- Circular stack contained in a metal pressure vessel
- 1.2 kW gross power input per module for GEO application
- Polymer membrane electrolyte (9 mil thick membranes)
- 150°F operating temperature
- 300 or 1800 psia maximum operating pressure
- 3.7 psia pressure during fuel cell discharge period
- .7% parasite power requirements

Reactant Tankage:

- Minimum storage pressure of 60 psia
- Metal tanks for a maximum pressure of 300 psia
- Composite tankage for 1800 psia operation

The system PEM fuel cell performance is taken from a GE report (Electrochemical Cell Technology for Energy Storage, ECDES-121, April 6, 1984). The performance assumes a relatively thin PEM membrane of 9 mils (wet), an operating temperature of 200°F, and an operating pressure of 30 psia. The 200°F temperature is the highest projected level consistent with the chosen cell materials and the required life expectancy for GEO application. Cell pressures above 30 psia would decrease the stack size but would put an increased pressure differential across the internal cell water separator plate.

The PEM electrolyzer performance data is consistent with a cathode water feed system operating at 150°F and 300 psia described in the GE report, "Electrochemical Cell Technology for Orbiter Energy Storage, ECOES-118, March 1984." Cathode water feed results in lower cell performance than that for anode feed, however, injecting the water at the anode results in significant water transport from the anode to the cathode due to protonic flow. If the ERP is sized for product water storage only, then during the electrolysis operation much water would be pumped to the cathode side and an ERP would be required to absorb this transferred water. Eventually the anode ERP would be depleted and the cell would operate as a cathode feed system. Using the cathode feed system directly permits the ERP on the anode side to be kept small in size. The cases studied for this system assumed an electrolysis cell potential of 1.5 volts. This voltage was chosen because it is close to the potential at which no cell waste heat is generated during electrolysis, however the heat of condensation must be rejected. The operating current density at this cell potential is only 25 amps per $ft^2$ for the cathode water feed cell and this is well within the water transport capabilities of the water storage ERP.

Previous studies have shown that operating the electrolysis cells at 1.5 volts is close to the weight optimum for a GEO energy storage system. Higher electrolysis cell voltages would result in higher current density operation and therefore smaller electrolysis cell stacks, however it would result in almost no change in the size and weight of the water storage ERP located in the electrolysis cell stack. Higher electrolysis cell voltages would require higher fuel cell voltages to maintain a constant system efficiency of 55%. Higher fuel cell voltages result in lower stack power densities with a subsequent increase in the stack size and weight. Since the fuel cell represents the majority of the system weight, the net effect of raising the electrolyzer voltage above 1.5 volts per cell is to increase the overall system weight. Reducing the electrolysis cell voltage below 1.5 volts would require adding heat to the electrolysis cell stack increasing the complexity and weight of the cooling system.

## C. Weight and Volume Summary

Figure 33 compares the weights and specific energy densities of two 12.5 kW modules operating at 55% efficiency for use in GEO satellite applications. The modules differ only in the method of stack cooling; i.e. graphite plates versus heat pipe coolers. The weights show a slight advantage to the heat pipe cooled system (363 vs. 407 lbs) mostly due to the weight difference in the electrolysis cell stacks (74 vs. 108 lbs). The heat pipe version is lighter because it can take advantage of a circular stack configuration for the electrolysis cell versus the annular arrangement required if a graphite cooler is used. The annular configuration is heavier than the circular option because it requires a bigger pressure vessel and more edge seal area. Neither of these two PEM dedicated system options achieved the goal specific energy of 50 watt-hrs/lb at 55% efficiency. The lightest system was the heat pipe version at 41.3 watt-hrs/lb. Higher system specific energies (lower weights) are possible for high pressure versions of this system which use composite tankage in place of metal tankage.

12.5 KW NET POWER OUTPUT PER MODULE
55% WHR EFFICIENCY
300 PSIA MAXIMUM OPERATING PRESSURE

| | GRAPHITE COOLERS | HEAT PIPE COOLERS |
|---|---|---|
| FUEL CELL STACK | 137 | 133 |
| ELECTROLYSIS CELL STACK | 108 | 74 |
| H2 & TANKAGE | 59 | 59 |
| O2 & TANKAGE | 44 | 44 |
| EXTERNAL CONDENSER | 0 | 0 |
| PRESSURE REGULATORS & VALVES | 18 | 18 |
| MISCELLANEOUS | 41 | 36 |
| **TOTAL LBS** | 407 | 363 |
| **WHRS/LB** | 36.9 | 41.3 |

105-170
872005

Figure 33. Dedicated PEM Energy Storage Systems Module Weight Breakdown

Figure 34 shows that the 50 watt-hrs/lb can only be achieved when both the reactant tankage and the PEM electrolysis stack pressure vessel are replaced by light weight composite tankage. One concern that must be investigated further is the impact on the heat transfer through the pressure vessel wall of the electrolysis cell stack when using composite materials for construction. The graphite fiber/resin mix of the composite has a lower thermal conductivity than the metal wall resulting in lower wall temperatures available to the external satellite cooling system. However, the higher pressure option, using composite tanks, lowers the weight 17% and reduces the system volume by more than a factor of 4 (Figure 35).

## D. Cell Stack Summary

All of the configurations studied for the dedicated PEM systems used the same low pressure (30 psia) fuel cell stack configuration as shown in Figure 36. It is basically modeled after the alkaline Orbiter powerplant in that it is a square cell stack using internal o-ring sealing instead of a containment pressure vessel. Gases

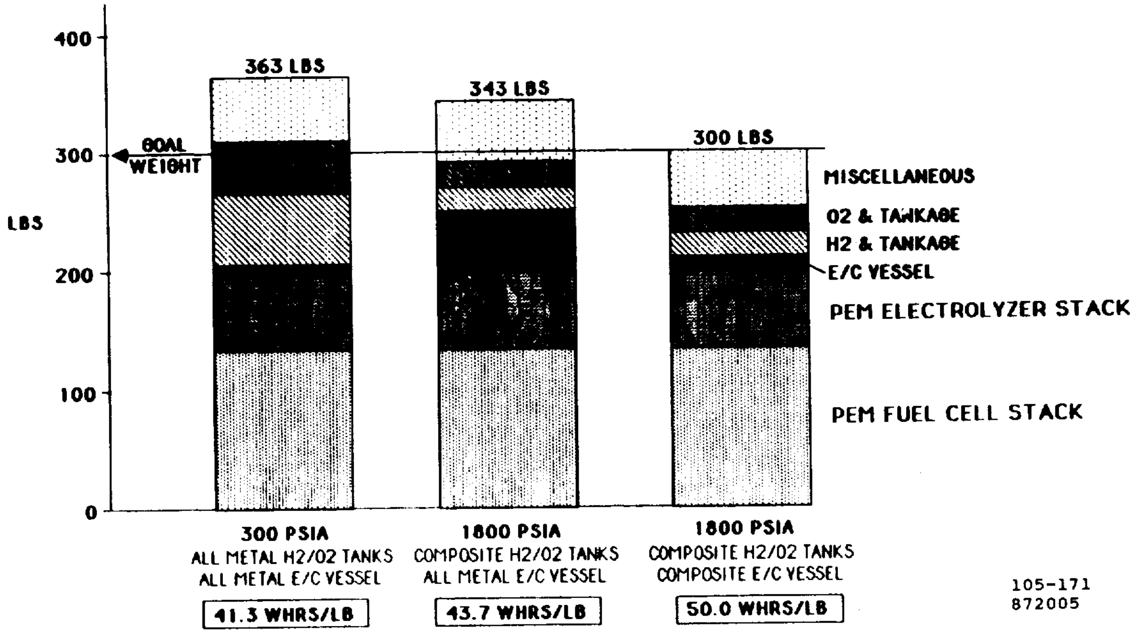

Figure 34. 12.5 kW Energy Storage System for GEO Satellite Application

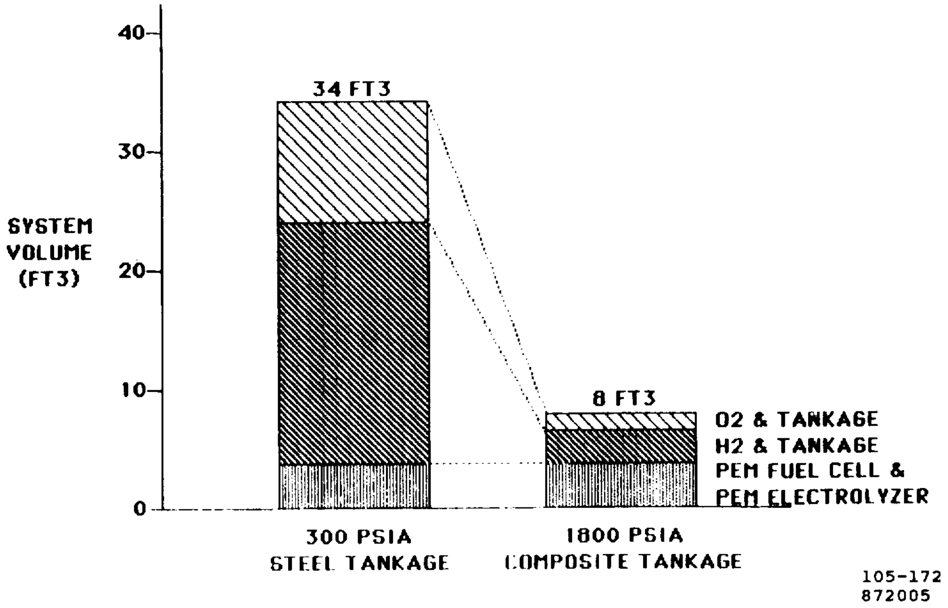

Figure 35. 12.5 kW Energy Storage System for GEO Satellite Application

are manifolded through passages located in the edge seal area surrounding the active cell area. The manifolded gases include $H_2$, $O_2$, and pure water vapor. The cooling plates consist of flat plate heat pipes located about every 6 cells. Details of heat pipe cooling are given in Section III of this report. The stack employs relatively simple bipolar current collection versus the somewhat less efficient and more complicated edge current collection imposed by the integrated stacks using interleaved fuel cell and electrolyzer cells. This system employs the same bipolar current collection as the dedicated alkaline system discussed in Section V. This does impose the requirement that the coolers which extend to the outside edge of the stack be electrically isolated from any attached cooling system. This could be done by use of a thin coating of a nonconductive elastomeric material, such as that proposed for use in the integrated, annular stack design discussed in Section IV. Figure 37 shows the internal detail of a single cell extracted from the stack. The plates forming the gas compartments, and the water separator are porous graphite, a compatible material at fuel cell potentials even in the oxidizing environment of the cathode. The water vapor separator consists of two graphite ERP's facing back to back separated by a fine pore graphite plate. The fine pore plate,

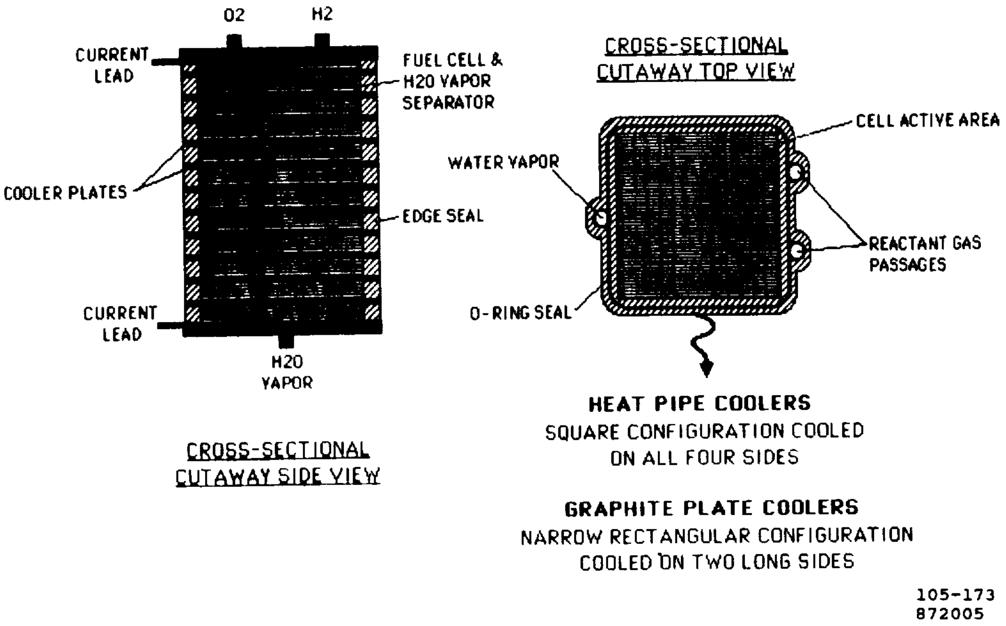

Figure 36. PEM Fuel Cell Stack

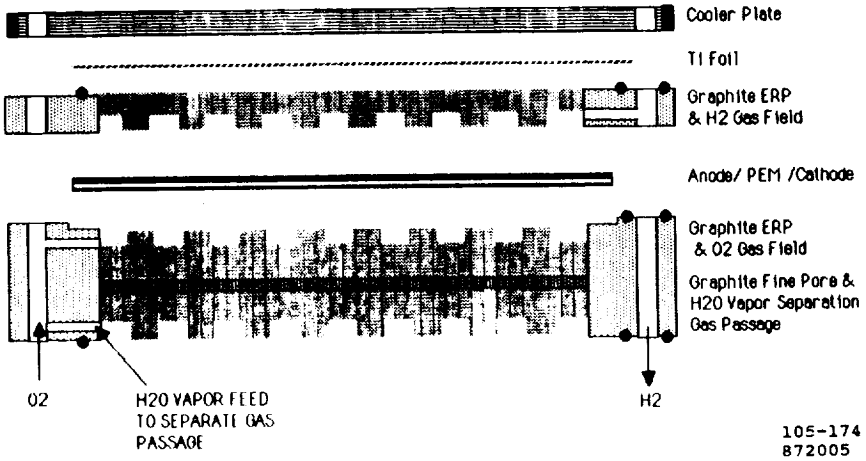

Figure 37. Cell Detail - PEM Fuel Cell

filled with liquid water (versus KOH/water in the alkaline system), maintains the pressure differential between the anode and water vapor compartments while the ERP's provide support, a path for current collection, and a reservoir to keep the fine pore plate wet during operational transients. The ERP's in the fuel cell stack are not required for storage of product water since it is actively removed from the stack and thus they can be designed to minimum thicknesses set mostly by structural and manufacturing considerations.

Figure 38 shows the heat pipe cooled version of the dedicated PEM electrolysis cell stack. This stack is a circular configuration contained in either a metal or composite material pressure vessel. The $H_2$ and $O_2$ gases are collected and manifolded through passages located in the stack edge seals. A separate water vapor manifold in the electrolysis stack is not required since the water vapor enters through the $H_2$ gas manifolding when the stack is inactive and at low pressure.

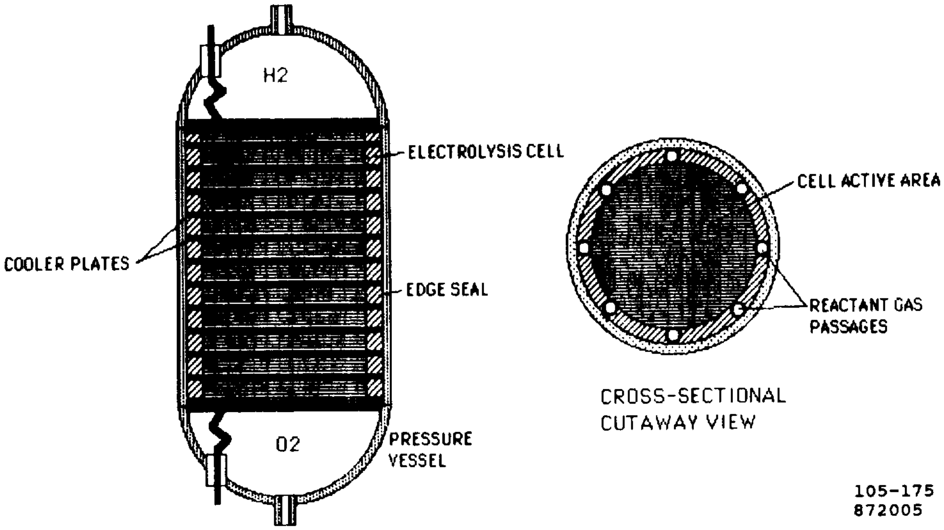

Figure 38. PEM Eletrolysis Cell Stack

Figure 39 shows a view of a single repeating element from the PEM electrolysis cell stack and two differences can be noted for this cell relative to the fuel cell. First, there is no water separation device but there is a large ERP required to store water supplied from the fuel cell stack during its discharge period. Second, the graphite ERP used in the fuel cell oxygen compartment has been replaced by a porous titanium ERP since the operating potentials of electrolysis are much higher and corrosion is more of a problem.

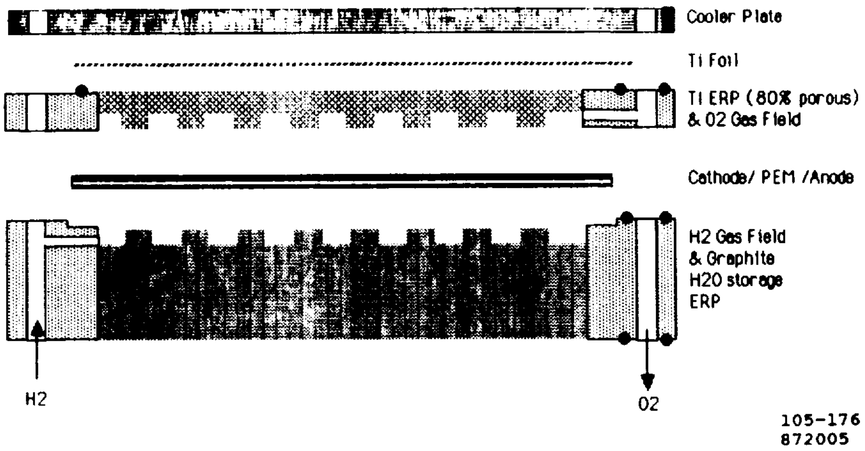

Figure 39. Cell Detail - PEM Electrolyzer

Figure 40 summarizes the design characteristics of both the fuel cell and electrolysis cell stacks for the baseline heat pipe cooled systems discussed in this section.

ORIGINAL PAGE IS
OF POOR QUALITY

**FUEL CELL STACK :**

12.5 NET POWER OUTPUT (END OF LIFE)
120 VOLTS PER STACK
.843 VOLTS PER CELL
127 AMPS PER FT2
.838 FT2 PER CELL (ACTIVE AREA)
142 CELLS PER STACK
CELL LENGTH = 11.5 INCHES (INCLUDES EDGE SEAL)
CELL WIDTH = 11.5 INCHES (INCLUDES EDGE SEAL)
STACK HEIGHT = 24 INCHES (INCLUDES END PLATES)
HEAT PIPE COOLERS EVERY 6 CELLS
BIPOLAR CURRENT COLLECTION

**ELECTROLYSIS STACK :**

1.2 GROSS POWER INPUT (END OF LIFE)
120 VOLTS PER STACK
1.5 VOLTS PER CELL
20 AMPS PER FT2
.5 FT2 PER CELL (ACTIVE AREA)
80 CELLS PER STACK
CELL DIAMETER = 10 INCHES (INCLUDES EDGE SEAL)
STACK HEIGHT = 20 INCHES (INCLUDES END PLATES)
HEAT PIPE COOLERS EVERY 6 CELLS
BIPOLAR CURRENT COLLECTION

**105-177**
**872005**

Figure 40. Dedicated PEM Cell Stack Summary

## VII. DUAL FUNCTION ALKALINE SYSTEM

### A. Description of Analysis Approach

The dual function system is an integrated alkaline stack concept in which each single cell functions as both a fuel cell and an electrolysis cell. This approach has the potential for achieving a number of system advantages. Primarily, product water storage and transfer are minimized. Secondly, the number of cells and associated system components is reduced, thus providing a potentially high reliability system. Thirdly, if a dual function cell could be developed, with high performance, system weight and energy density would be very attractive for satellite applications. And finally in some configurations the $H_2$ and $O_2$ reactants could be incorporated into the same pressure vessel as the stack, thus reducing volume.

To date, the difficulty in developing a system of this type is the incompatibility of high performance fuel cell oxygen electrode catalysts, when operating in the electrolysis mode. Most fuel cell catalysts are not stable at potentials of interest during electrolysis operation. Electrolysis oxygen catalysts operate poorly in the fuel cell mode. Therefore, the synthesis of an oxygen catalyst with stability and reasonable performance during both modes of operation would be a highly desirable goal.

To indicate the potential advantages of this system a parametric study was conducted showing the impact of fuel cell performance, specific weight (lbs/ft$^2$) and operating pressure on overall system energy density (watt-hours/lb.).

Figure 41 shows a schematic of the dual function system consisting of a hydrogen tank, oxygen tank, and dual function cell stack contained in a pressure vessel. The cell stack itself consists of the dual function cells, graphite or heat pipe cooler plates, graphite ERP's for storage of the product water, endplates, current collectors, and edge seals containing the reactant gas manifolds. The exact sizes and weights of these stack components and the stack pressure vessel cannot be

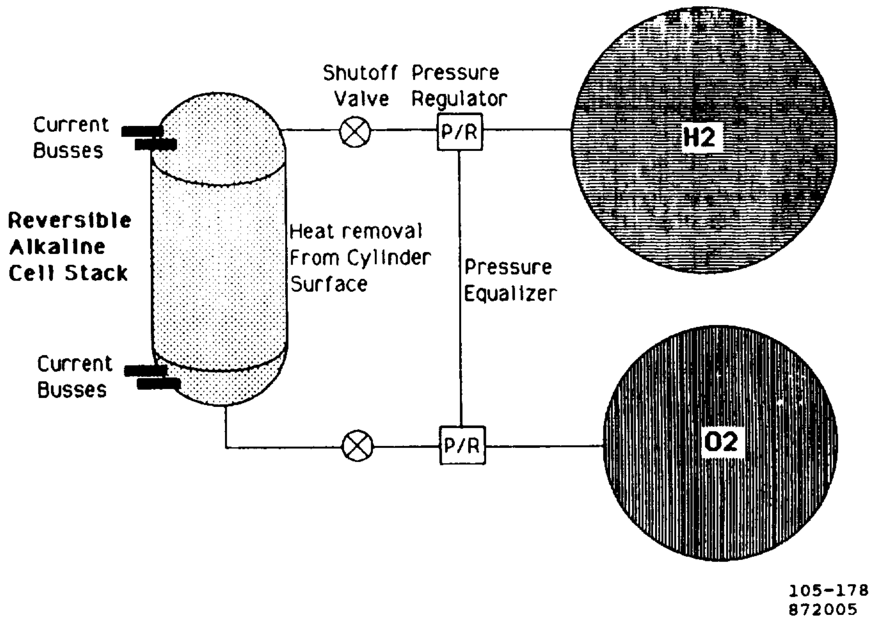

Figure 41. Dual Function Alkaline Energy Storage System

determined until the cell performance is known, for it is the fuel cell performance which determines the cell stack configuration. For a 55% efficient GEO satellite application the cell stack operates in a fuel cell mode for a maximum 1.2 hours followed by the electrolysis cell mode of operation for a minimum of 22.8 hours. The fuel cell must output a full 25 kW of power during discharge (two 12.5 kW modules) while the electrolysis cell requires only about 2.4 kW of input power over the 22.8 hour recharge period. Because of the vast difference in power requirements the optimum system weight for a given efficiency is achieved when the reversible cell stack design is based on the fuel cell mode of operation. For this analysis the fuel cell performance was varied parametrically relative to the performance of an advanced Orbiter alkaline fuel cell operating at 60 psia and 180°F. For a given performance level the power density, cell voltage, and stack thermal characteristics are known and the cell configuration including the amount of active cell area and the number of cells per stack can be calculated. Other factors which determine the final stack weight include the thickness and density of cell components including cells, edge seals, endplates and coolers. The cell stack specific weight is the sum of the weights of the dual function cells and their coolers per square foot of active cell area and it does not include the weights of endplates, the water storage ERP's, or the external pressure vessel. The cell stack specific weight is a function of the cell stack design including the types of materials used in its construction and the thickness of the cell components. Lighter cell specific weights are representative of higher technology designs using thinner and lighter cell components. This study used the fuel cell component weights and materials based on an advanced Orbiter cell design which was constructed and tested under a contract with JSC. The impact on cell component weights (i.e. lbs/cell + coolers), when deviating from this design, was studied in a parametric fashion.

## B. Results of the Parametric Analysis of the Dual Function System

Figure 42 shows the specific energy of a reversible alkaline energy storage system as a function of the cell and cooler specific weight (lbs/ft$^2$) for three system options:

1. An 1800 psia system with composite $H_2$, $O_2$ and stack tankage.
2. An 1800 psia system with composite $H_2$, $O_2$ tankage and metal stack tankage.
3. A 300 psia system with all metal $H_2$, $O_2$ and stack tankage.

These systems were designed for a 55% efficiency and assumed that the dual function cell had the same performance as a dedicated alkaline fuel cell.

Overlayed on this chart is the estimated specific weight of the cells and heat pipe coolers of a dual function system whose components were based on the advanced Orbiter technology stack. The figure shows that for this design, both high pressure options (1 and 2) exceeded the specific energy goal of 50 watt-hrs/lb and the all metal tankage option (3) falls just below the goal. The figure also shows that reducing the weight of the cell and cooler components could result in system specific energies approaching 100 watt-hrs/lb. This would require cell/cooler specific weights less than 1 lb/ft$^2$.

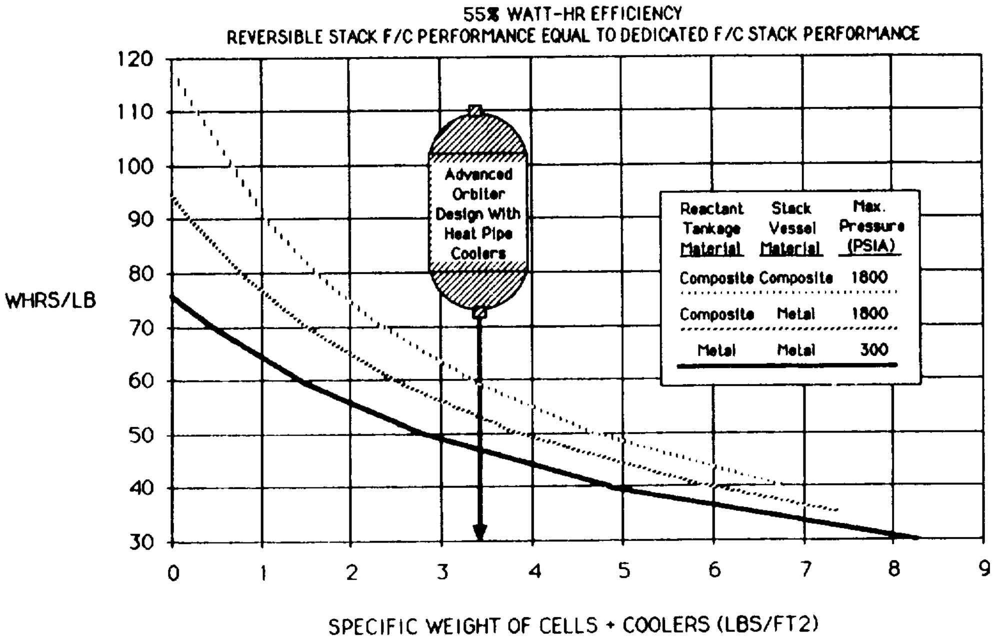

105-179
872005

Figure 42. Dual Function Alkaline Energy Storage Systems System Specific Energy vs Cell/Cooler Specific Weight

These results assumed that the fuel cell performance was equal for dual function and dedicated alkaline stacks while Figure 43 shows the impact of not achieving the same level of fuel cell performance in a dual function stack. The advanced Orbiter technology system would be 12% heavier for all three tankage and system pressure options if the actual dual function cell performance proved to be 100 mv below the reference fuel cell performance. At this lower performance level only the all composite tankage option, operated at 1800 psia, has a system specific energy density exceeding the goal of 50 Whrs/lb.

The dual function cell stack system has the following general characteristics:

Circular cells in a pressure vessel
Heat pipe coolers located approximately every 5 cells
12.5 kW net power output per module
120 volts nominal output

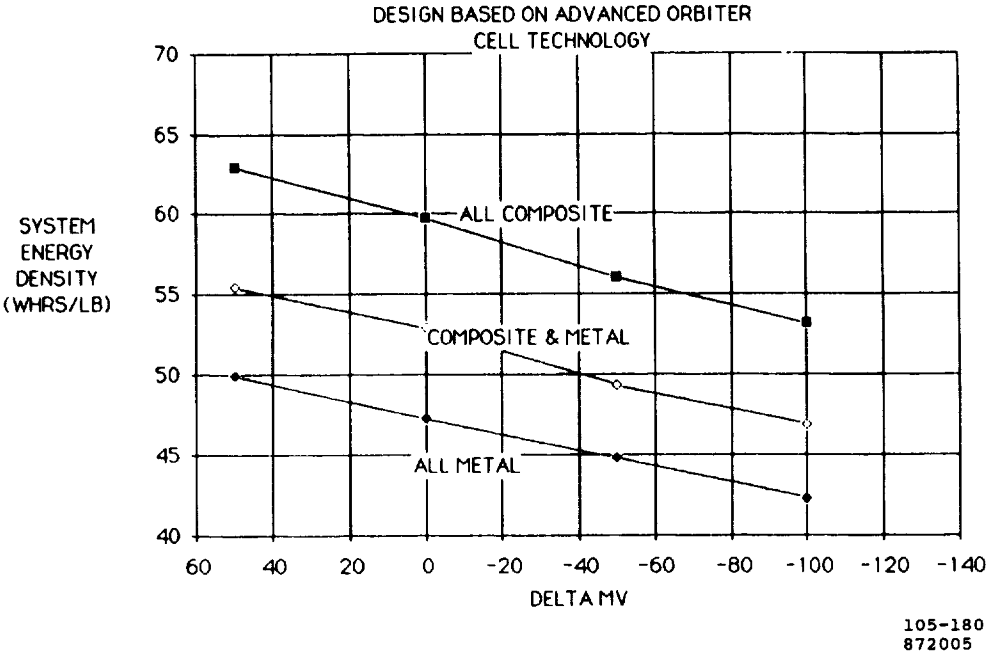

Figure 43. Dual Function Alkaline Energy Storage System

Alkaline electrolyte - 32% KOH, 68% water
180°F operating temperature
Operating pressures:
  1800 - 60 psia with composite reactant tankage
  300 - 60 psia with all metal reactant tankage
Water storage in an internal ERP
Fuel cell mode parasite power - 1.5%
Electrolysis cell mode parasite power - 0.67%

The cell used in this system is shown in Figure 44. It consists of an anode gas passage formed from a porous graphite plate. The plate has 20 mils of graphite with 50% slotted open for gas passages, and 10 mils of porous graphite plate without slots. These thicknesses are chosen to keep the plates as light as possible while still providing the good structural integrity, reasonable current collection paths, and adequate flowpaths for the reactant gases. The water storage ERP adjoins the cathode passage ERP and has a thickness dependent on the amount of water stored, the number of cells per stack, and the active area per cell. The gas passage on

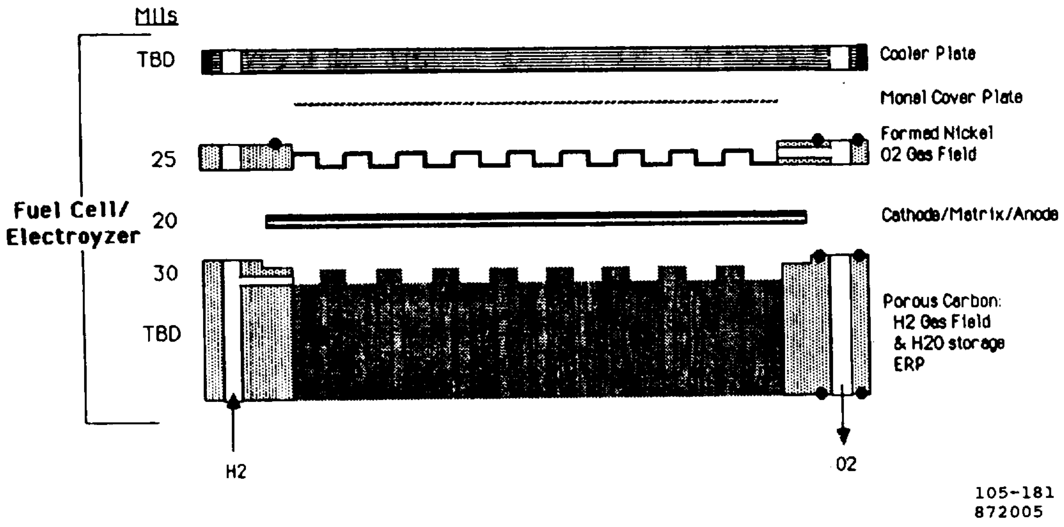

Figure 44. Cell Detail - Dual Function Alkaline Fuel Cell/Electrolyzer

the $O_2$ side of the stack is constructed of a formed nickel sheet required to prevent corrosion during the electrolysis cell mode of operation. The matrix containing the anode and cathode catalyst layers is 20 mils thick, the same matrix thickness as in the advanced Orbiter alkaline stack. The final element of the cell is the heat pipe cooler chosen instead of a graphite cooler plate to permit the use of a circular cell stack configuration, thereby minimizing the size and weight of the containment pressure vessel.

Figure 45 shows the cell stack schematic which indicates several key features. The reactant gases are manifolded through gas passages located in the edge seal area of the circular stacks. The current collection is from plates on either end of the stack due to the bipolar configuration of the stack compared to the edge current collection scheme required in the integrated annular stack analyzed in Section IV of this report. Heat removal in this stack is through the wall of the pressure vessel with heat pipe cooler plates carrying the heat from the cells to the wall. Finally, the cell stack is arranged as two substacks to facilitate the series-parallel electrical connections required when switching from fuel cell to electrolysis cell operation. The substacks are connected in parallel during the electrolysis cell mode to provide the higher stack potentials required for its operation (120 volts across each substack).

A very advanced version of the dual function cell energy storage system was analyzed to determine the minimum weight of such a system using reasonable extrapolations of stack and materials technology. The resulting system achieved a specific energy of 115 watt-hrs/lb. The technology assumptions included raising the fuel cell temperature from 180°F to 300°F which tends to increase the cell performance and results in a smaller, lighter cell stack. Some conservatism was applied to the stack design in that it was assumed that the dual function stack operating as a fuel cell had 50 millivolts lower performance than an equivalent dedicated fuel cell stack. The fuel cell and cooler specific weight for this advanced system options was assumed to be 1 lbs/ft$^2$. Designs as low as 0.34 lbs/ft$^2$ have been conceived for high power density cells and if only a portion of these improvements can be incorporated it should be possible to reduce the cell/cooler specific weight from 3.4 lbs/ft$^2$ to 1 lb/ft$^2$. In addition to the stack improvements lighter weight composites are being developed for pressure vessels using ultra thin welded metal liners. These advanced composite tanks are more than 40% lighter than the composite high pressure gas storage tanks incorporated in the balance of this report. These advanced technology concepts combine to give a system with a specific energy density of 115 watt-hrs/lb.

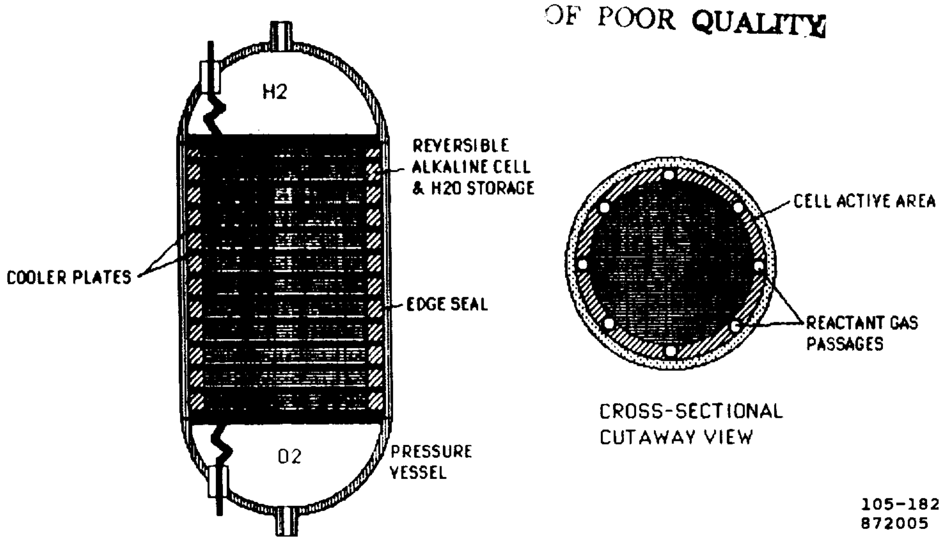

Figure 45. Dual Function Alkaline Cell Stack

# VIII. RELIABILITY

At the present time the most extensive data base available, dealing with the failure rate of individual fuel cells, comes from the experience gained during the field test program conducted by IFC from 1981 to 1986 on 46 power plants. Each unit was designed to deliver 40 kW of power, and was tested in a commercial environment and maintained by local personnel. The program was oriented toward achieving economic viability and as such the fuel cells did not have the extensive quality control or pre-operational testing that one would expect for an aerospace power plant.

Results from this program, based on over 80 million cell hours of operation indicated that there was not one stack shutdown caused by a cell failure in the open mode. Based on these results and using standard reliability analysis techniques, it is possible to calculate a cell failure rate that must be less than .01 failures per million hours ($.01 \times 10^{-6}$). Failures which would cause stack shutdowns, will be some fraction of this value.

For this study, it has been assumed that to achieve the desired reliability a completely redundant regenerative fuel cell module, including reactant supply system, would be carried on-board. The Air Force has specified a reliability goal of .995 for their advanced battery studies. Using a cell failure rate of .002 failures per million hours, a value that would appear to be achievable, the reliability of a complete system can be determined. Using published failure rates of $.08 \times 10^{-6}$ HRS$^{-1}$ for the cell stack containment vessel, the reliability of the integrated alkaline system is calculated to be .989. This is somewhat short of the Air Force goal, and to insure the .995 level means that the system life would be limited to 7 years.

For a reversible alkaline cell, and using the same failure rate as above ($.002 \times 10^{-6}$ HRS$^{-1}$) fewer cells are required and a reliability of .995 can be achieved over a 10 year period. For this analysis a performance penalty of 20% was used for the reversible stack compared to the level used for the integrated system. Thus from a reliability consideration, the reversible stack concept is the favored approach.

National Aeronautics and Space Administration

# Report Documentation Page

| | | |
|---|---|---|
| 1. Report No.<br>NASA CR-179609 | 2. Government Accession No. | 3. Recipient's Catalog No. |
| 4. Title and Subtitle<br>Regenerative Fuel Cell Study for Satellites in GEO Orbit | | 5. Report Date<br>July 1987 |
| | | 6. Performing Organization Code |
| 7. Author(s)<br>Alexander Levy, Leslie L. Van Dine, and James K. Stedman | | 8. Performing Organization Report No.<br>FCR-8347 |
| | | 10. Work Unit No.<br>506-41-21 |
| 9. Performing Organization Name and Address<br>International Fuel Cells Corporation<br>195 Governors Highway, P.O. Box 739<br>South Windsor, Connecticut 06074 | | 11. Contract or Grant No.<br>NAS3-22234 |
| | | 13. Type of Report and Period Covered<br>Contractor Report<br>Final |
| 12. Sponsoring Agency Name and Address<br>National Aeronautics and Space Administration<br>Lewis Research Center<br>Cleveland, Ohio 44135 | | 14. Sponsoring Agency Code |

15. Supplementary Notes

Project Manager, Olga D. Gonzalez-Sanabria, Power Technology Division, NASA Lewis Research Center.

16. Abstract

This paper summarizes the results of a 12-month study to identify high performance regenerative hydrogen-oxygen fuel cell concepts for geosynchronous satellite application. Emphasis was placed on concepts with the potential for high energy density (W-hr/lb) and passive means for water and heat management to maximize system reliability. Both polymer membrane and alkaline electrolyte fuel cells were considered, with emphasis on the alkaline cell because of its high performance, advanced state of development and proven ability to operate in a launch and space environment. Three alkaline system concepts were studied. The first, termed the integrated design utilized a configuration in which the fuel cell and electrolysis cells are alternately stacked inside a pressure vessel. Product water is transferred by diffusion during electrolysis operation and waste heat is conducted through the pressure vessel wall, thus using completely passive means for transfer and control. The second alkaline system, referred to as the dedicated design, uses a separate fuel cell and electrolysis stack so that each unit can be optimized in size and weight based on its orbital operating period. The third design was a dual function stack configuration, in which each individual cell can operate in both the fuel cell and electrolysis mode, thus eliminating the need for two separate stacks and associated equipment. Results indicate that using near term technology energy densities between 46 and 52 W-hr/lb can be achieved at efficiencies of 55 percent. Using advanced lightweight cell construction which has been achieved in experimental cells, composite tankage material for the reactant gases and the reversible stack concept, system energy densities of 115 W-hr/lb can be projected.

| | |
|---|---|
| 17. Key Words (Suggested by Author(s))<br>Hydrogen-oxygen fuel cells<br>Geosynchronous orbit<br>Alkaline fuel cells | 18. Distribution Statement<br>Unclassified - unlimited<br>STAR Category 44 |

| 19. Security Classif. (of this report) | 20. Security Classif. (of this page) | 21. No of pages | 22. Price* |
|---|---|---|---|
| Unclassified | Unclassified | 81 | A05 |

NASA FORM 1626 OCT 86 *For sale by the National Technical Information Service, Springfield, Virginia 22161